UNITED NATIONS EDUCATIONAL, SCIENTIFIC AND CULTURAL ORGANIZATION
INTERNATIONAL CENTRE FOR THEORETICAL PHYSICS
I.C.T.P., P.O. BOX 586, 34100 TRIESTE, ITALY, CABLE: CENTRATOM TRIESTE

SMR.780 - 38

FOURTH AUTUMN COURSE ON MATHEMATICAL ECOLOGY

(24 October - 11 November 1994)

"Carbon Biogeochemistry and Climate Change"

Jorge L. Sarmiento
Atmospheric and Oceanic Sciences Program
Princeton University
Princeton, NJ 08544
U.S.A.

and

Michael Bender
Graduate School of Oceanography
University of Rhode Island
Kingston, RI 02881
U.S.A.

Photosynthesis Research **39**: 209–234, 1994.

Minireview

Carbon biogeochemistry and climate change

Jorge L. Sarmiento[1] & Michael Bender[2]
[1] *Atmospheric and Oceanic Sciences Program, Princeton University, Princeton, NJ 08544, USA;*
[2] *Graduate School of Oceanography, University of Rhode Island, Kingston, RI 02881, USA*

Received 14 October 1993; accepted in revised form 26 November 1993

Key words: carbon biogeochemistry, climate change, carbon cycle, atmospheric CO_2 content

Abstract

The rapid increase of atmospheric CO_2 resulting from anthropogenic activites has stimulated a great deal of interest in the carbon cycle. Important decisions need to be made about future tolerable levels of atmospheric CO_2 content, as well as the land and fossil fuel use strategies that will permit us to achieve these goals. The vast amount of new data on atmospheric CO_2 content and ancillary properties that has become available during the last decade, and the development of models to interpret these data, have led to significant advances in our capacity to deal with such issues. However, a major continuing source of uncertainty is the role of photosynthesis in providing a sink for anthropogenic emissions. It is thus appropriate that a new evaluation of the status of our understanding of this issue should be made at this time.

The aim of this paper is to provide a setting for the papers that follow by giving an overview of the role of carbon dioxide in climate, the biogeochemical processes that control its distribution, and the evolution of carbon dioxide through time from the origin of the earth to the present. We begin with a discussion of relevant processes. We then proceed to a more detailed discussion of the time periods that are best documented: the late Pleistocene (during which time large continental ice sheets waxed and waned) and the modern era of anthropogenic impact on the carbon cycle.

The greenhouse effect

The Earth receives short-wavelength radiation emitted from the sun, and re-radiates this energy to space at longer wavelengths. In the absence of an atmosphere, the Earth's surface temperature would be fixed at that value where the surface of the planet radiated heat to space at the same rate as it intercepts heat from the sun. This temperature is given by the equation $Q = \sigma T^4$, where Q = heat flux, σ = Stefan–Boltzmann constant, and T = temperature (degrees Kelvin), and is equal to 256 K. The higher value of the Earth's average temperature, 288 K, reflects the fact that water vapor, CO_2, methane, ozone, and other radiatively active gases in the atmosphere absorb radiation emitted at the Earth's surface then re-emit radiation from within the atmosphere. Earth's equilibrium radiative temperature is thus reached in the atmosphere at some elevation well above the Earth's surface. Because air is compressible, the atmosphere warms as one descends from this elevation to the surface. Temperature at the surface of the earth is thus 32 K warmer than the radiative equilibrium temperature.

The flux of energy emitted to space from the Earth's surface is a strong function of wavelength. Figure 1 shows the flux as a function of wavelength for a site with a surface temperature of 294 K. The solid line is the calculated radiation flux for a clear-sky with the effect of greenhouse gases included. The minimum in outgoing radiation centered at 15 μm is due to

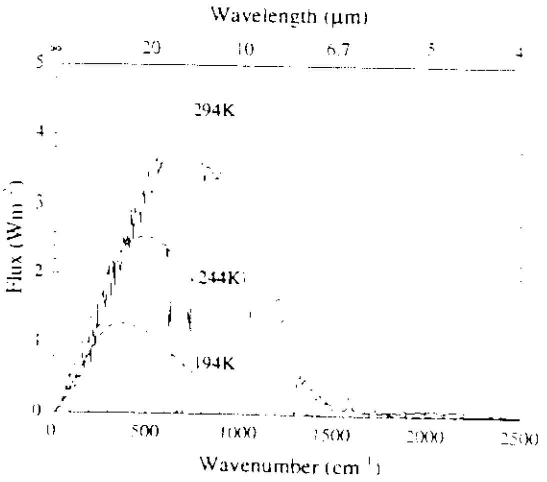

Fig. 1. Outgoing clear-sky terrestrial radiation calculated by K.P. Shine for a region where the surface temperature is 294 K (Shine et al. 1990). The dashed lines show the hypothetical energy flux which would be observed if none of the outgoing radiation were intercepted in the atmosphere.

absorption by CO_2, and that near 9 to 10 μm is due to absorption by ozone. Emission to the atmosphere of trace gases which absorb radiation at wavelengths where the atmosphere is now transparent have an important effect on the radiative balance even at very low levels of concentration. The atmospheric CO_2 concentration, on the other hand, is already absorbing most of the radiation in its absorption band. A proportionally larger increase in the atmospheric CO_2 burden is thus necessary to significantly affect the radiative balance of the atmosphere, which would be achieved by increasing the absorption towards the edges of the band. The relative efficiencies of the major greenhouse gases, expressed as forcing per molecule normalized to CO_2, are given in Table 1.

Anthropogenic activities are increasing atmospheric burdens of the naturally occurring radiatively active gases CO_2, CH_4, and N_2O, as well as chlorofluorocarbons which are produced industrially and do not occur in nature. The changes in the contributions of each of these gases to the radiative balance of the atmosphere due to their concentration increases between 1765 and 1990 are summarized in Table 1. Despite its high background concentration, CO_2 is being added in such large amounts that it accounts for about 61% of the enhanced capacity of the atmosphere to absorb long wavelength radiation emitted from the surface. CH_4 and N_2O account for about 27% of the total anthropogenic radiative forcing, and chlorofluorocarbons for the remaining 12%. Because of its primary role in anthropogenic forcing of the Earth's radiative balance, a great deal of effort is being invested in understanding the biogeochemistry of CO_2, its role in natural climate changes of the Earth during geologic time, and the ways CO_2 is released to, and removed from, the atmosphere at the present time.

Table 1. Effect of various anthropogenic gases on the radiative balance of air. Middle column: efficiency of radiative forcing, expressed as a function of absorption per added molecule, with $CO_2 = 1$. Right-hand column: changes in radiative forcing between 1765 and 1990 due to increasing concentrations (Shine et al. 1990). The methane forcing change also includes the indirect effect due to formation of water vapor in the stratosphere

Gas	Normalized forcing per added molecule	Forcing change 1765–1990 (W m^{-2})
CO_2	1	1.50
CH_4	21	0.56
N_2O	206	0.10
CFC-11	12 400	0.062
CFC-12	15 800	0.14
Other CFCs		0.085
		2.45

Carbon cycle processes

Time scales of 10^6 to 10^9 years

The Earth, along with the rest of the solar system, formed 4.6×10^9 years before present by the accretion of gases and particles which were concentrated in our region of space. During and after its accretion, two processes worked to enrich the surface of the planet in the volatile elements and compounds (H_2O, CO_2, N_2, noble gases) which are present in much higher abundances on the surface than in the interior of the planet. The first was differential accretion, with volatiles accumulating last, after most of the planet had formed, and hence being concentrated at the surface (e.g., Chyba 1987). In the extreme case, this process would cause the Earth

2.

to start out with its atmosphere and ocean intact, although not necessarily with their current chemical configuration. The second process is Earth degassing, in which tectonic phenomena such as volcanism transfer volatiles from the Earth's interior to the ocean and atmosphere throughout geological time. This process too is capable of producing high atmospheric CO_2 levels early in the Earth's history.

How high was the atmospheric CO_2 concentration early in Earth's history? A constraint comes from the climate of the planet and the evolution of the sun. Almost since its formation, the sun's heat has derived from hydrogen burning (a series of nuclear reactions in which 4 protons and 2 electrons are transformed into a ^{4}He nucleus and energy). As the H/He ratio of the sun has dropped, the sun has decreased in size and given off progressively more heat, raising the rate at which heat is received at the Earth's surface. The luminosity of the young sun was about 25% less than today, requiring that the Earth's greenhouse effect early in the history of the solar system should have been much greater than today if, as thought, water was present at the surface (e.g., Kasting 1985). Kasting (1985) and others, who have argued that CO_2 was probably always responsible for most of the greenhouse effect not due to water vapor (today water vapor is the dominant greenhouse gas), have constrained the CO_2 concentration early in Earth's history as the level necessary to raise the temperature of much of the planet above 0 °C. In this way, Kasting (1985) estimated that the CO_2 concentration of the young Earth was 80–600 times the present value.

The subsequent evolution of the atmospheric CO_2 concentration is a matter of much speculation. The last 560×10^6 years of Earth history has been more extensively studied than earlier times. Three types of observations suggest large variations of CO_2 during this time (Fig. 2), as well as a link between high CO_2 and warm climates. The first type involves various techniques for directly estimating past atmospheric CO_2 levels. Cerling and others have studied the $\delta^{13}C$ of $CaCO_3$ and organic carbon deposits found in soils (Cerling et al. 1991, Cerling 1991, Mora et al. 1991, and Cerling 1992). $\delta^{13}C$ expresses variations in the abundance ratio of the rare, heavy, stable isotope of carbon, ^{13}C (~1.1 atom %), to the other stable isotope ^{12}C (~98.9 atom %). It is presented in units of permil (‰), defined by the formula:

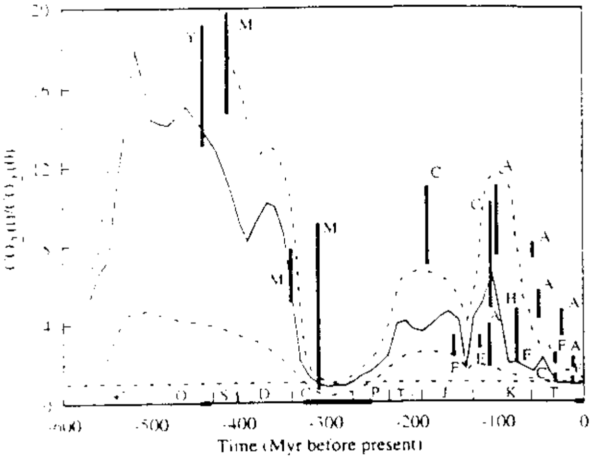

Fig. 2. The ratio of Phanerozoic atmospheric carbon dioxide to the present level plotted versus time (Berner 1992). The solid line and dashed uncertainty lines are from the theoretical model of Berner (1991). The horizontal bars along the abscissa indicate periods of glaciation, which coincide with low CO_2 levels except during the late Ordovician. The vertical bars are various estimates of paleo-CO_2 levels (Y = Yapp (1992); M = Mora et al. (1991); C = Cerling (1991); F = Freeman and Hayes (1992); A = Arthur et al. (1991); H = Hollander and McKenzie (1991)).

$$\delta^{13}C \text{ (per mil)} = [(^{13}C/^{12}C)_{sample}/(^{13}C/^{12}C)_{std} - 1] \times 10^3$$

The $\delta^{13}C$ of soil CO_2 is intermediate between the atmospheric value of about −6.5‰ and the value of about −26‰ in CO_2 which is released by respiration of C-3 plants (C-4 plants, which have a smaller fractionation, did not come into being until the Miocene; Thomason et al. 1988). $\delta^{13}C$ values closer to air indicate that the CO_2 concentration of air was high in the past, while $\delta^{13}C$ values closer to organic matter indicate that atmospheric CO_2 was low. The $\delta^{13}C$ of CO_2 in soil gas is sometimes imprinted in the $\delta^{13}C$ of $CaCO_3$ precipitated in soil. The difference between the $\delta^{13}C$ of these $CaCO_3$ deposits and their associated organic carbon deposits holds a clue to past variations in the concentration of CO_2 in air. The data along this line have been interpreted as indicating that the atmospheric

3.

CO_2 concentration during the Cretaceous Era ($\sim 100 \times 10^6$ years before present) was 5 to 11 times higher than today. The soil results for the Cretaceous are confirmed by measurements of $\delta^{13}C$ in organic matter and $CaCO_3$ deposits in ocean sediments (e.g., Freeman and Hayes 1992). The difference between these reflects photosynthetic fractionation, which is observed to be significantly lower in low CO_2 waters, and higher in high CO_2 waters. An additional constraint comes from the fact that the concentration of CO_3^{2-} in the mineral goethite (FeOOH) depends on the cocentration of CO_2 in air. Using this contraint, Yapp (1992) suggested that atmospheric carbon dioxide content at 440×10^6 years was ~ 16 times higher than today.

The second general approach to estimating past levels of atmospheric CO_2 comes from modeling. Berner et al. (1983), Lasaga et al. (1985), Berner (1991), and others built a mathematical model of the global CO_2 cycle to hindcast the variation of CO_2 through time (Fig. 2). The basic processes invoked by this model involve the organic carbon cycle of burial in sediments and subsequent exposure to weathering as part of the great tectonic (mountain-building) cycles within the Earth, and the silicate cycle outlined in simplified form in Fig. 3. $CaCO_3$ and SiO_2 are produced as skeletal material in the oceans and precipitated in marine sediments. This material is buried deeply within the Earth and heated. $CaCO_3$ and SiO_2 are transformed to $CaSiO_3$ and CO_2 in the process known as metamorphism. The CO_2 thus produced percolates through the Earth's crust to the atmosphere, resulting in a CO_2 flux to air that is proportional to the rate of tectonics. Meanwhile, metamorphic rocks (represented by $CaSiO_3$) are uplifted back to the Earth's surface, where they are decomposed by attack of the CO_2 in air. This decomposition (termed weathering) consumes CO_2 and produces Ca^{2+}, HCO_3^-, and SiO_2 which dissolve in rivers and flow back to the oceans. The rate of weathering will rise as the CO_2 concentration increases, due primarily to the warming that results from the CO_2 increase. This simple negative feedback will force CO_2 to that level where removal by weathering equals input of CO_2 to the atmosphere by tectonic processes. Climate will thus be warmest during times when tectonic cycles are most intense. Data reflecting past rates of sea floor spreading indicate that the Cretaceous and the period between the Cambrian and Devonian Epochs ($\sim 550 \times 10^6$ to 350×10^6 years before present) were such times (Gaffin 1987). Berner (1991) shows that the high CO_2 levels of the Cretaceaous are due primarily to the high spreading at that time, with an enhanced effect due to the predominance of more rapidly recycled deep water carbonates after the Jurassic ended about 150×10^6 years ago (Wilkinson and Walker 1989).

The development of vascular plants during the Silurian–Devonian about 400×10^6 years ago and of angiosperms during the Cretaceous about 130×10^6 years ago (Taylor and Hickey 1990) are thought to have led to a significant increase in weathering rate (Volk 1989). The increase resulted from higher soil CO_2 levels, which today are about 5000 to 10 000 ppmV (Brook et al. 1983), greatly in excess of the atmospheric level of 350 ppmV. The direct feedback between atmospheric CO_2 and weathering rate is thus very small today, as contrasted with the indirect feedback through greenhouse warming. The situation prior to the advent of vascular plants probably involved a stronger direct feedback.

Berner's (1991) simulations led him to conclude that the drop in atmospheric CO_2 levels that occurred during the Carboniferous and the generally lower levels since then are due primarily to the advent of vascular plants.

The third refers to strong evidence, based on studies of plant and animal fossils, that climate in mid-latitude and high latitude regions during the Cretaceaous was much more equable than today (Barron 1983). Barron and Washington (1985), among others, have used sophisticated climate models to investigate what factor(s) may have caused these warmer climates. They concluded that the only plausible explanation was a greater greenhouse effect induced by past atmospheric CO_2 concentrations about 4 times higher than at present.

The tectonic, weathering, and evolutionary processes invoked in the long term carbon cycle models fix the mean levels of CO_2 which must be attained over periods of millions of years. How-

4.

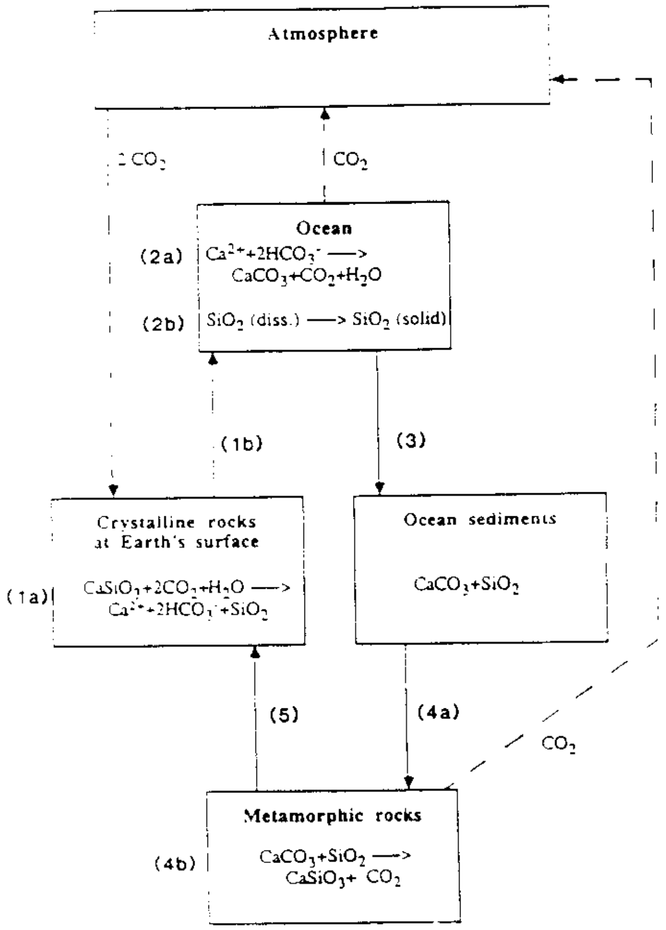

Fig. 3 A highly simplified representation of the link between geochemical processes and average CO_2 concentration of air on a time scale of 10^6 years or longer. Key processes are: (1) 'weathering' of crystalline rocks at the Earth's surface (the decomposition of crystalline rocks by carbon dioxide to give cations, HCO_3^-, and SiO_2 which are then transported to the oceans by rivers); (2) precipitation of skeletal $CaCO_3$ and SiO_2 by marine organisms; (3) incorporation of skeletal material into marine sediments; (4) burial and heating of sediments and the consequent chemical transformations known as metamorphism; and (5) uplift of crystalline metamorphic rocks to the Earth's surface to complete the cycle.

ever, natural fluctuations about these mean levels are possible: they can be induced by changes in ocean circulation and biological carbon cycling. We now turn our attention to the question of how oceanic processes can cause variations in the CO_2 concentration of air.

Time scales of 10^2 to 10^6 years

Among the most remarkable aspects of the CO_2 distribution is that the vast majority of the combined atmosphere and ocean inventory is in the oceans: 98.5% prior to the industrial revolution (Fig. 4) and 98.1% today. By contrast, a more typical atmospheric gas such as O_2 has only 0.6% of its combined atmosphere and ocean inventory in the ocean. Because of this unique behavior of CO_2, natural levels of atmospheric pCO_2 are controlled almost entirely by oceanic processes on a time scale of about 10^2 to 10^6 y. In this section we discuss the relevant oceanic processes and the potential for them to be modified by biology and climate change.

One reason for CO_2's unique behavior is that, due to hydrogen bonding, CO_2 is very soluble in water (e.g., CO_2 is about 30 times as soluble as O_2). However, the primary reason is that the vast majority of dissolved CO_2 exists in the

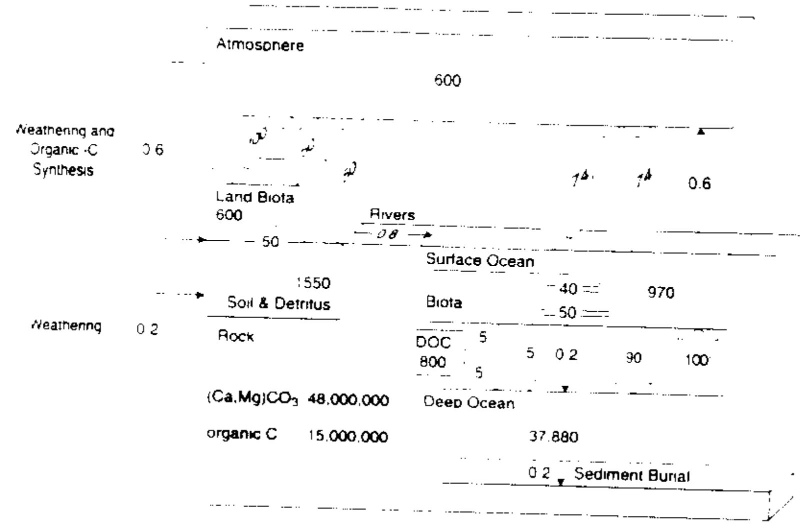

Fig. 4 The pre-industrial carbon budget based on IPCC (Watson et al. 1990) as modified by Sarmiento and Siegenthaler (1992) and Siegenthaler and Sarmiento (1993). The numbers inside the boxes are inventories in Pg (10^{15} g) of carbon, and the fluxes are Pg carbon per year. DOC is dissolved organic carbon.

hydrolyzed and dissociated forms, as bicarbonate and carbonate ions. Global mean surface sea water (temperature of 17.64 °C, salinity of 34.78 parts per thousand by weight, alkalinity of 2.311 milliequivalents per kg, and total carbon of 2.002 millimoles per kg) has only 0.5% of its total carbon as CO_2. Bicarbonate ion and carbonate ion account for the remaining 88.8% and 10.7%, respectively.

The concentration of the total dissolved inorganic carbon (DIC, which is the sum of CO_2 and bicarbonate and carbonate ions) in the oceans is about 12% higher below 1 km depth than at the surface. This increase of total DIC with depth is an extremely important feature of ocean chemistry. About 3% of the 12% difference is due to the fact that CO_2 is more soluble in the cold deep waters which fill the abyss than in warmer surface waters. The 'solubility pump' (Volk and Hoffert 1985) is effected by release of CO_2 to the atmosphere from warm waters at low latitudes, poleward transport through the atmosphere, and uptake by cold water at high latitudes. The cold carbon rich high latitude waters are dense, primarily because of their temperature, and sink into the abyss. These deep waters fill the abyssal ocean below a few hundred to a thousand meters below the sea surface, all the way to the ocean floor at a mean oceanic depth of 4000 meters.

The remainder of the increase of DIC with depth in the oceans is due to biology. Organic matter produced by photosynthesis in the euphotic zone (upper ~100 meters) is exported to the abyss by sinking of large particles. It also reaches the deep sea by passive transport of dissolved organic matter and suspended particles in waters mixed and advected downward into the ocean interior. The vast majority of this organic matter is re-mineralized by bacteria. In this process CO_2 is 'pumped' from surface water to deep water by the combined effects of photosynthesis, sinking and respiration.

How do the biological and solubility pumps affect the air-sea flux of CO_2? Perhaps the most important point to emphasize is that these pumps involve fluxes in carbon from one reservoir to another. If the fluxes in and out of a given reservoir are not in equilibrium, the amount of CO_2 in that reservoir will change through time. Later we show atmospheric CO_2 data which demonstrate a near constant concentration for a millenium prior to the industrial revolution. Based on these data we believe that the biological and solubility pumps were in a near steady state which involved no significant global

net
los
riv
sca
to
pu
of
int
the
T
air-
not

Fig.
(198
area
Herr

net flux across the air-sea interface except for the loss required to balance the net inflow from rivers (see Fig. 4). In other words, on a global scale, the carbon being removed from or added to the surface by the biological and solubility pumps must be balanced primarily by transport of carbon *within* the ocean, not across the air-sea interface. The nature of this flux is discussed in the next paragraph.

The requirement for no net flux across the air-sea interface must be satisfied globally, but not necessarily locally. Thus, the solubility pump drives a flux of CO_2 from low latitude to high latitude waters. The biological pump also has a major impact on air-sea fluxes. The excess total inorganic carbon content of the deep ocean that results from the input due to the biological pump is continually transported back to the surface by upwelling, convective overturning driven by wintertime cooling, and mixing. Figure 5 shows the locations where the two most important of these processes, upwelling and wintertime convective overturning, predominate. Biological uptake eventually strips out the excess carbon that

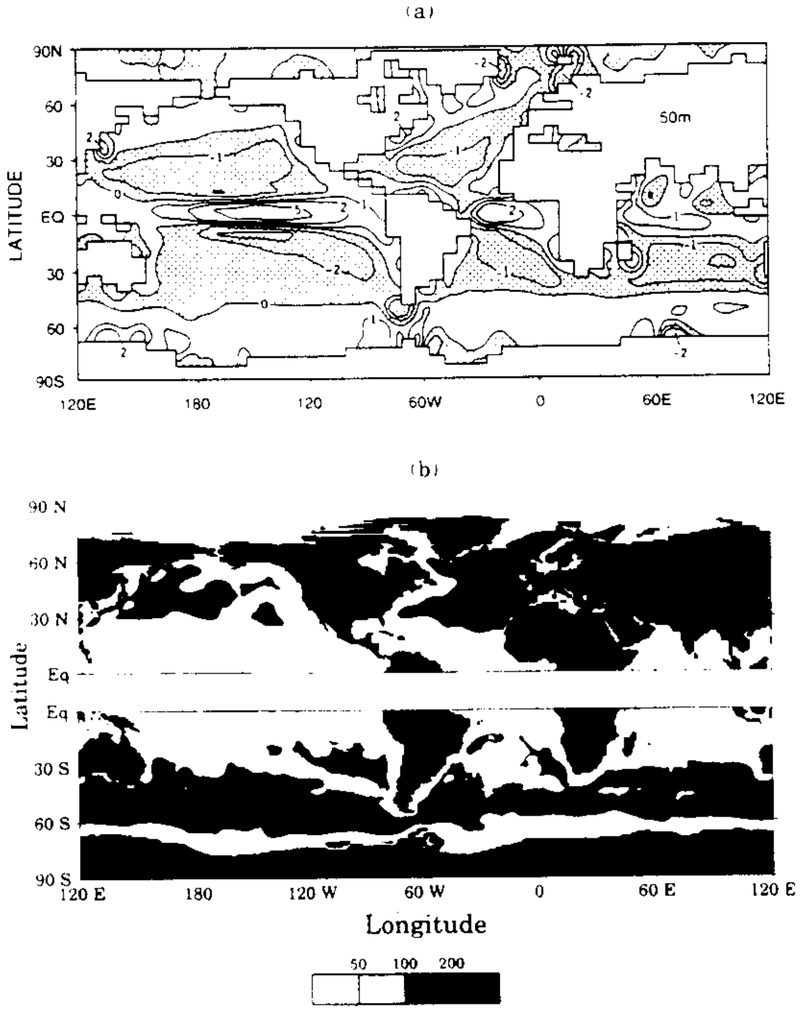

Fig. 5. (a) Upwelling velocity at a depth of 50 meters as determined by the ocean general circulation model of Toggweiler et al. (1989) forced with the annual mean climatic winds of Hellerman and Rosenstein (1983). Units are 10^{-6} m s^{-1}, with downwelling areas indicated by stippling. (b) Depth of the wintertime mixed layer (January, February, and March in the Northern Hemisphere; July, August, and September in the Southern Hemisphere) as estimated by Levitus (1982). Units are m.

arrives at the surface, thus closing the steady state conveyor belt. However, on the average, the upwelling and deep convection regions tend to have excess carbon levels at the surface, in part because it takes time for the biology to strip it all, and in part because other processes limit the efficiency of photosynthetic uptake in some of these regions. The overall result is a large flux of CO$_2$ out of the Equatorial regions due to the combined effect of warming and the upwelling of waters rich in excess carbon. In high latitude regions the solubility pump uptake which results from cooling is counteracted in many places by upwelling and deep convective input of waters rich in excess carbon. The subtropical gyres are generally regions of cooling and downward advection of water. Thus they usually take up CO$_2$ from the atmosphere. All these features are illustrated in the estimated air-sea CO$_2$ difference map of Takahashi shown in Fig. 6.

One of the consequences of the continual addition of DIC to deep ocean water by re-

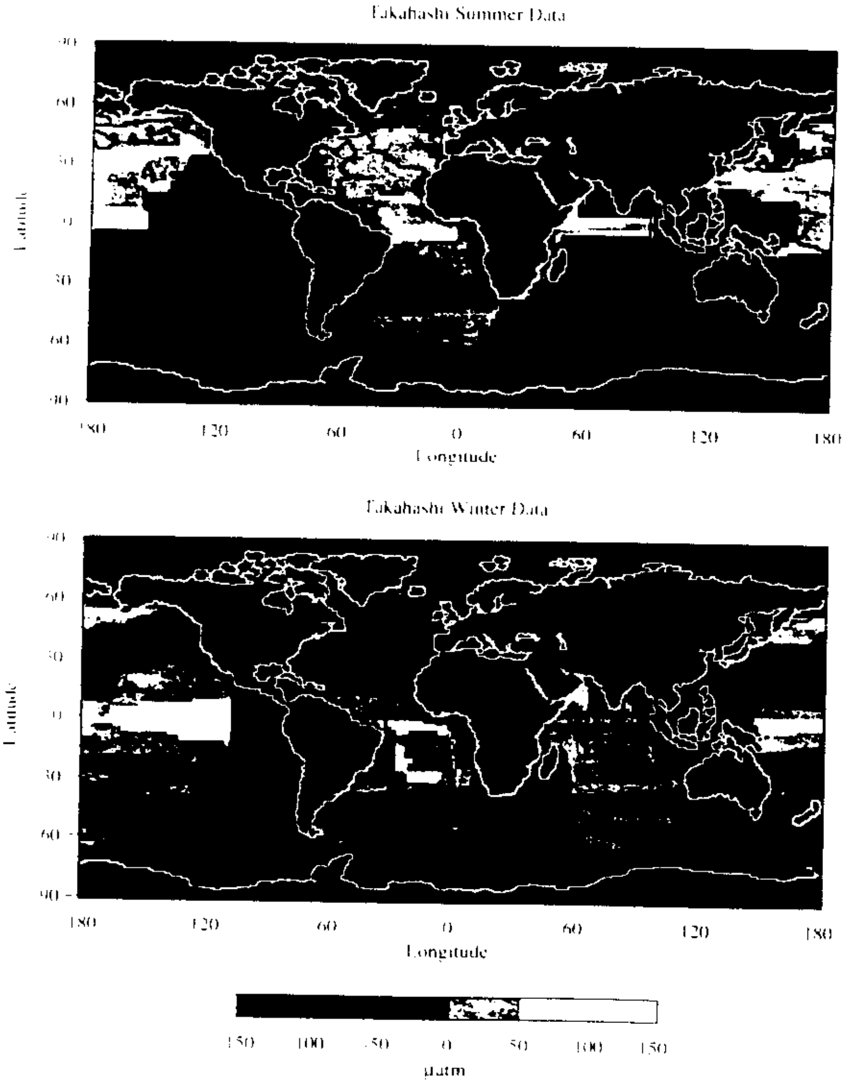

Fig. 6. Map of the mean sea-air CO$_2$ difference in ppmV (produced by T. Takahashi based on measurements: Tans et al. 1990). The dark line indicates the 0 contour. Areas of positive difference have a flux from the ocean to the atmosphere, negative areas have a flux from the atmosphere to the ocean.

mine
have
total
of th
deep
highe
An
biolo
is in
photo
solve
the
lowe

**Fig. 7.
Oceans
in the
concen
Ocean.
carbon**

mineralization is that the oldest ocean waters have the highest DIC concentrations. Thus, the total carbon concentration is in effect a snapshot of the global ocean circulation, with the oldest deep Pacific waters (age ~10^3 y) having the highest concentrations in the world (Fig. 7).

An intriguing irony of ocean chemistry and biology is that the concentration of total carbon is in great excess over that which is utilized by photosynthesis, yet the concentration of dissolved CO_2, which is the form of carbon used in the carboxylation reaction with RuBisCO, is lower than that required for maximum efficiency of this reaction. However, oceanic phytoplankton on the whole appear to have evolved mechanisms to compensate for this deficiency (Raven 1994).

What then does limit the uptake of total carbon by phytoplankton in the surface ocean? Ocean biogeochemists look first to the supply of the major nutrients, phosphate and nitrate. The surface map in Fig. 8 shows that phosphate is depleted nearly everywhere in the surface ocean except in the North and Equatorial Pacific and a vast region in the Southern Ocean. A nitrate map would be very similar. Thus, a finite major

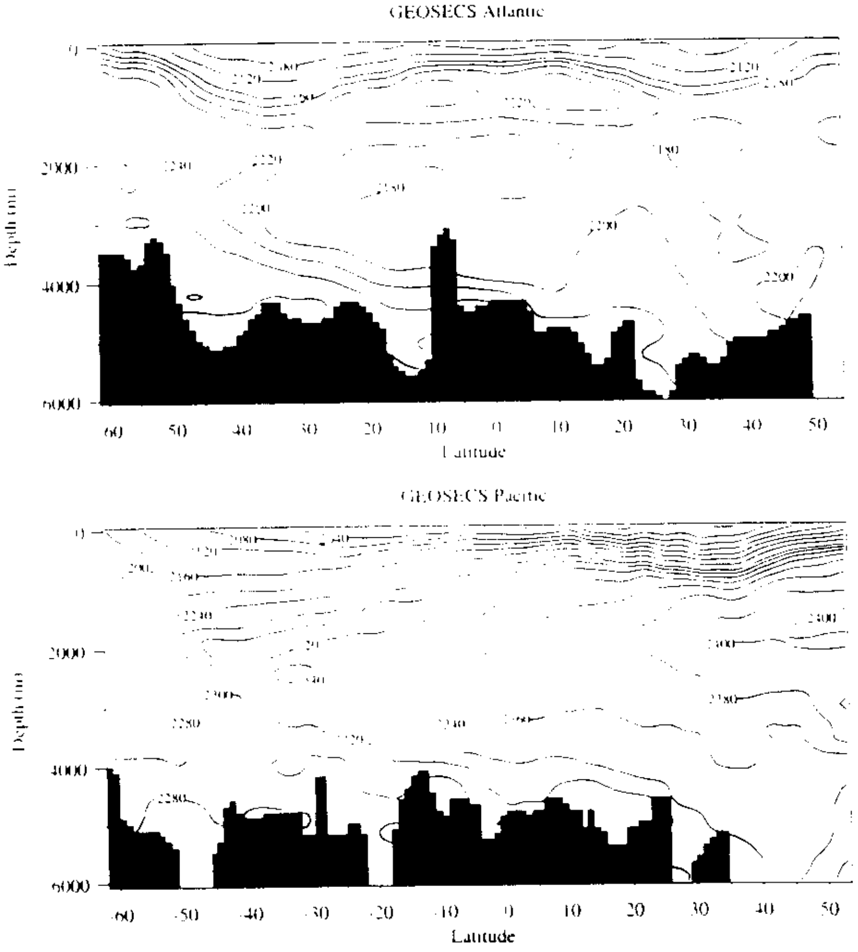

Fig. 7. North-south total total dissolved inorganic carbon (DIC) sections in the western Atlantic (Bainbridge 1976) and Pacific Oceans (Craig et al. 1981). The contour interval switches from 40 mmol kg^{-1} below 2180 mmol kg^{-1} to 20 above 2180 mmol kg^{-1} in the Atlantic. In the Pacific the switch in contour interval occurs at 2280 mmol kg^{-1}. Note the increase in deep water concentrations as one progress southwards from the regions of fresh deep water formation in the North Atlantic to the Southern Ocean, and then northwards to the oldest deep waters at intermediate depth in the North Pacific. This results from the addition of carbon by remineralization of organic matter.

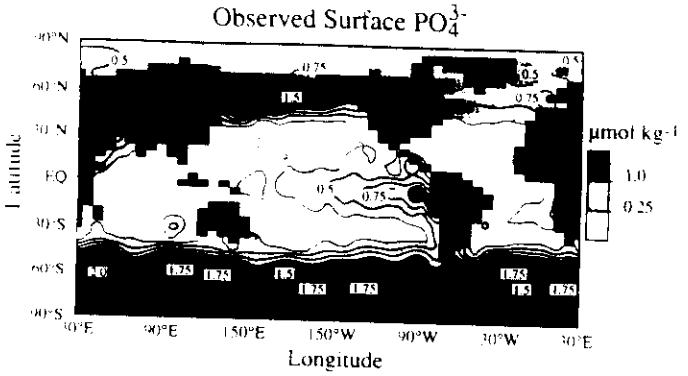

Fig. 8. Map of mean phosphate concentration in mmol L^{-1} at the surface of the ocean as determined from a global data set by Levitus et al. (1993). The countour interval is 0.25 mmol L^{-1} with changes in shading every 0.50 mmol L^{-1}. The global mean phosphate is 2.15 mmol L^{-1}.

nutrient supply can explain the limited uptake of total carbon over most of the ocean. We do not yet know why uptake of the major nutrients is incomplete in other regions. A number of hypotheses exist and are being actively explored, as discussed in the paper by Falkowski in this issue (Falkowski 1994).

It is interesting to examine how the ocean-atmosphere carbon balance would be affected if the biological pump were to be altered. Such speculations are not idle. Alterations of the biological pump are the most likely explanation for documented modifications of atmospheric pCO_2 that have occurred in the past 10^5 years, and it has been suggested that they may play a role in future modifications. The results of a range of scenarios for alterations of the biological pump are summarized in Table 2. These scenarios investigate the impact of depleting nutrients in the four major regions of the world where they are high. We emphasize two major aspects of these results: (1) of the high nutrient regions, the Southern Ocean biological pump has by far the largest effect on the atmosphere-ocean carbon balance. The reason for this is that it is through the surface waters of the Southern Ocean that the vast majority of sea water, the cold dense waters of the abyss, come into contact with the atmosphere. (2) Changes in the Southern Ocean biological pump can alter atmospheric pCO_2 between a lower limit of 165 ppmV and an upper limit of about 450 ppmV, compared with the pre-industrial level of 280 ppmV. As we shall see, these alterations are within the range of recent (order 10^5 year) variations, but as the upper portion of Table 2 shows, they are relatively modest compared to scenarios of the anthropogenic increase over the next century.

An important consequence of the large oceanic capacity for CO_2 is that atmospheric pCO_2 is strongly buffered by oceanic processes on the several century time scale of ocean circulation. If, for example, enough CO_2 were added to the atmosphere (e.g., from the terrestrial biosphere or fossil fuel burning) to double the CO_2 content from its pre-industrial value of 600 Pg, only 104 Pg would remain there, bringing the total to 704 Pg. The remaining 496 Pg would be taken up by the ocean, at which point the atmosphere and ocean would be in equilibrium, except for the slow reaction of oceanic CO_2 with $CaCO_3$ in ocean sediments ($CO_2 + CaCO_3 + H_2O = Ca^{2+} + 2HCO_3^-$).

However, this uptake would occur over a relatively long time scale. Oceanic uptake of such a pulse occurs in two steps. The first is gas exchange across the air-sea interface. This process results in equilibration between the atmosphere and the surface mixed layer (the upper few tens of meters of the ocean which winds continuously stir and homogenize). The second is vertical exchange of the surface mixed layer with interior waters of the ocean. Although the surface mixed layer equilibration takes longer for CO_2 than for other comparable gases due to the fact that so much of the carbon is in the form of

---

Table 2.
nutrient
Business
over the r
The ΔpC

Scenario

IPCC Bu
(1) Bas
(2) Eff
(a) S
(b) N
(c) N
(d) E
Box mod
Biologi
Off
Part
Full

bicarb
enough
uptake
with in
The
mixed
using
circula
lation
Hassel
The re
CO_2 c
value
oceani
that c
tial te
found
the o
prima
18.9%
of 10.
years.
The r
until
begin
This r
to tak
even
is be
uptak
phere
large

10

Table 2. Sensitivity of atmospheric pCO_2 to the oceanic biological pump: scenarios of the impact on atmospheric pCO_2 of surface nutrient depletion for various regions that have high surface nutrients today (Sarmiento and Orr 1991). The baseline IPCC Business as Usual Scenario has an increase in atmospheric pCO_2 content to about 785 ppmV from its present value of 355 ppmV over the next 100 years. The ΔpCO_2 values shown for the IPCC scenarios represent the impact of 100 years of nutrient depletion. The ΔpCO_2 values shown for the box models are for models that are run out to equilibrium over a period of a few thousand years

Scenario		ΔpCO_2 (ppmV)
IPCC Business as Usual (1990–2090)		
(1) Baseline		+430
(2) Effect of nutrient depletion on top of baseline		
(a) Southern Ocean	(south of 31.12° S)	−71.8
(b) North Atlantic	(31.12° N − 80.06° N)	−12.7
(c) North Pacific	(31.12°N − 66.69° N)	−6.9
(d) Equatorial Region	(17.78°S − 17.78° N)	−2.8
Box models of impact of Southern Ocean biological pump		
Biological pump:		
Off (no stripping of nutrients)		+170
Partial (pre-industrial scenario, for which pCO_2 = 280 ppmV)		0
Full (all nutrients stripped out)		−115

bicarbonate and carbonate ions, it is still fast enough that the rate limiting step to oceanic uptake is vertical exchange of the mixed layer with interior waters.

The rate of vertical exchange between the mixed layer and interior waters has been studied using three dimensional models of the general circulation of the oceans (Ocean General Circulation Model or OGCM; Maier-Reimer and Hasselmann 1987, and Sarmiento et al. 1992). The results of studies in which the atmospheric CO_2 content was doubled from its pre-industrial value of 600 Pg carbon show that the rate of oceanic CO_2 uptake decreases with time in a way that can be approximated by a sum of exponential terms. In their study, Sarmiento et al. (1992) found that 5.4% of the CO_2 pulse is taken up by the oceans with a mean life of 0.9 years due primarily to equilibration with the mixed layer. 18.9% of the remainder enters with a mean life of 10.7 years, 30.7% with a mean life of 67.7 years, and 27.5% with a mean life of 376.6 years. The remaining 17.4% stays in the atmosphere until the excess CO_2 dissolved in the ocean begins to react with $CaCO_3$ in ocean sediments. This reaction increases the capacity of the oceans to take up CO_2 and reduces the airborne fraction even further (Broecker and Takashashi 1977). It is because of the long time scale of oceanic uptake that the release of CO_2 to the atmosphere by fossil fuel burning is leading to such a large increase in atmospheric pCO_2. At present, about 46% of the net anthropogenic CO_2 addition to the atmosphere by fossil sources and the terrestrial biosphere is airborne and 29% is in the ocean (Table 3).

What is the potential role of the terrestrial carbon reservoir in all this? On time scales in excess of 10^2 to 10^3 years, any carbon released or taken up by the terrestrial biosphere will have only a relatively modest impact on atmospheric CO_2. This is because of the strong diluting effect of the oceans. However, on shorter time scales the slow oceanic uptake does permit the terrestrial biosphere to play a significant role, which probably accounts for the missing sink in Table 3.

Warming of sea water causes the dissociation of HCO_3^- to CO_2 and CO_3^{2-} and a decrease in

Table 3. The 1980 to 1989 anthropogenic CO_2 budget: based on IPCC (Watson et al. 1990) with the atmospheric increase modified per Peter Tans (personal communication) and ocean error modified per Siegenthaler and Sarmiento (1993)

	Average perturbation (Pg/yr of C)
Sources to atmosphere	
(1) Fossil	5.4 ± 0.5
(2) Changes in land use	1.6 ± 1.0
Total	7.0 ± 1.2
Sinks	
(1) Atmosphere	3.2 ± 0.1
(2) Oceans	2.0 ± 0.6
Total	5.2 ± 0.6
Missing sink	1.8 ± 1.3

the solubility of CO_2. Warming thereby partitions CO_2 into the atmosphere. However, the CO_2 uptake capacity of the large oceanic reservoir is relatively insensitive to this direct impact of climate change. The partial pressure of CO_2 increases by about 4.3% for every degree change in sea water temperature. Thus the global mean equilibrium warming of 2.5 °C which models predict for an atmospheric pCO_2 doubling from 280 to 560 ppmV would release on the order of 60 ppmV to the atmosphere, increasing the atmospheric load by only 11%.

Time scales of 10^0 to 10^2 years

Monthly observations of atmospheric CO_2 display the remarkable pattern of seasonal oscillations illustrated in Fig. 9. There is a great richness of detail in these data. Most noteworthy is the almost continuous increase in magnitude of the seasonal oscillation with increasing latitude to the north, superimposed on the global increase in the CO_2 concentration of air due largely to the burning of fossil fuel. The seasonal oscillation is due primarily to terrestrial biological processes. During late spring and the summer atmospheric CO_2 is drawn down by a positive net biological production. During the fall, winter, and early spring the release of CO_2 to the atmosphere by decaying organic matter exceeds photosynthetic uptake, and atmospheric CO_2 rises. The low magnitude of the signal in the Southern Hemisphere is a result primarily of the small land area relative to ocean. The northwards increase in the signal in the Northern Hemisphere is due in part to increasing climate seasonality, and in part to the increasing predominance of land over ocean.

Biological production in the ocean is also highly seasonal and comparable in magnitude to terrestrial production (Fig. 4). Seasonality of ocean biology results from seasonal changes in the supply of light due to the angle of the sun (lower in winter), the depth of the mixed layer, and the supply of nutrients by seawater mixing and advection. Fall and winter cooling of the surface mixed layer in many high latitude regions of the ocean leads to de-stabilization and convective overturning to depths exceeding those at which light is adequate to support positive net growth of phytoplankton ($\geqslant \sim 100$ m; cf. Fig. 5 of mixed layer depth). This deep mixing also primes the biological pump by bringing up a fresh supply of nutrients that can be utilized once the mixed layer shallows and sun angle rises so that the light supply becomes adequate. The nutrient rich waters are also carbon rich. Thus the overall effect of mixed layer deepening is to enrich surface waters with CO_2. During spring and summer the mixed layer becomes stabilized and shallows. This permits photosynthesis to increase and take up the new nutrients as well as the CO_2 that was brought up from below.

In most regions of the ocean the seasonal variations in temperature play an even greater role in the seasonality of the ocean carbon

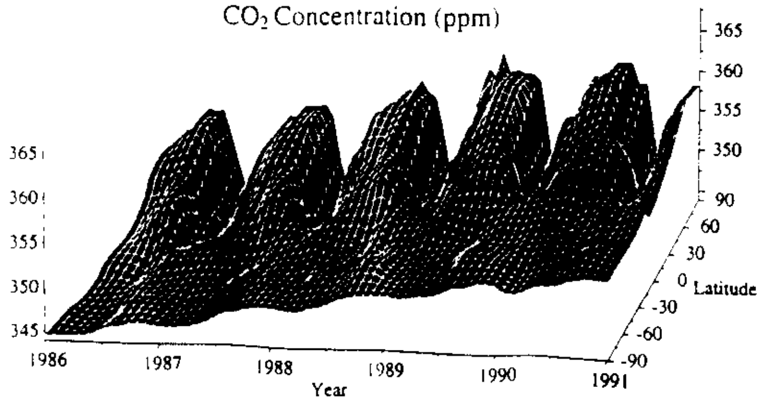

Fig. 9. Smoothed atmospheric CO_2 data as measured by the National Oceanic and Atmospheric Administration, Climate Monitoring and Diagnostics Laboratory's Flask Sampling Program (Conway et al. 1991).

system than does biology. The direct impact of temperature on carbon chemistry gives a 4.3% reduction in the saturation partial pressure of CO_2 for every degree centigrade of warming. Some of the CO_2 that is present in water before a warming occurs thus becomes available for evasion into the atmosphere. Cooling has the opposite effect. The indirect effect of temperature on the carbon cycle through its impact on ocean biology has been empirically determined by Eppley (1972), who gave a relationship for the temperature sensitivity of the maximum growth rate of phytoplankton which shows a range of ~ 7 over the entire oceanic temperature range of about 30 °C. Locally the range in temperature and growth rate would be far smaller. We have found in model simulations that this temperature effect has only a modest impact on new production.

The overall impact of these seasonal changes on the partial pressure of CO_2 in the ocean mixed layer can be quite large (e.g., Fig. 10), but, as previously noted, very little of this signal actually affects the atmosphere. The small impact of ocean seasonal process on the atmospheric seasonal signal is a consequence of the effect of carbon chemistry on the time scale for CO_2 equlibration between the atmosphere and ocean. The flux of a gas into or out of the ocean contributes to the surface mixed layer concentration of that gas (defined as C) according to the following time dependent equation:

$$\frac{\partial C_{ocean}}{\partial t} = \frac{k}{D_{ML}}(C_{atmosphere} - C_{ocean})$$

k is the gas exchange coefficient and D_{ML} the thickness of the mixed layer at the surface of the ocean. $(k/D_{ML})^{-1}$ defines a time constant which is the e-folding equilibration time scale for the mixed layer with respect to the atmosphere. The global mean of k is estimated to be 17.5 cm h^{-1} from radiocarbon measurements (Siegenthaler 1986). For a typical mixed layer of thickness 50 m, the time scale for equilibration would thus be about 12 days.

However, for $C = CO_2$, the above equation becomes:

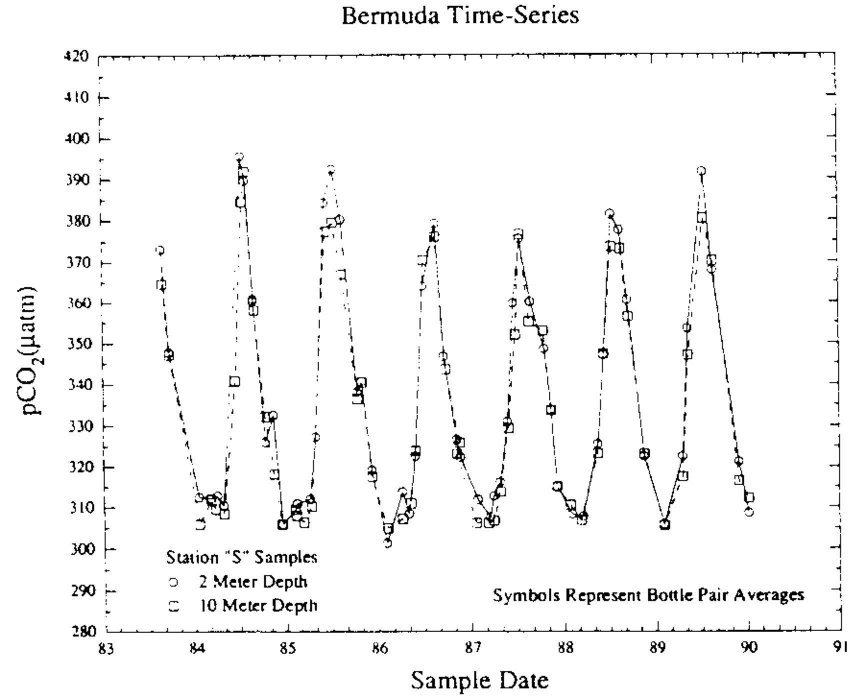

Fig. 10. Surface ocean carbon dioxide partial pressure off Bermuda as calculated by C.D. Keeling (personal communication) from DIC, alkalinity, temperature and salinity measurements.

$$\frac{\partial \mathrm{DIC}}{\partial t} = \frac{\partial \mathrm{DIC}}{\partial \mathrm{CO}_{2\mathrm{ocean}}} \cdot \frac{\partial \mathrm{CO}_{2\mathrm{ocean}}}{\partial t}$$

$$= \frac{\mathrm{k}}{\mathrm{D}_{\mathrm{ML}}} (\mathrm{CO}_{2\mathrm{atmosphere}} - \mathrm{CO}_{2\mathrm{ocean}}) .$$

i.e.,

$$\frac{\partial \mathrm{CO}_{2\mathrm{ocean}}}{\partial t} = \left(\frac{\partial \mathrm{DIC}}{\partial \mathrm{CO}_{2\mathrm{ocean}}} \right)^{-1}$$

$$\times \frac{\mathrm{k}}{\mathrm{D}_{\mathrm{ML}}} (\mathrm{CO}_{2\mathrm{atmosphere}} - \mathrm{CO}_{2\mathrm{ocean}})$$

where DIC is the total concentration of the three forms of inorganic carbon which are in chemical equilibrium with each other, namely CO_2, and the carbonate and bicarbonate ions (Najjar 1992). The equilibration time scale for $\mathrm{CO}_{2\mathrm{ocean}}$ thus becomes $(\partial \mathrm{DIC}/\partial \mathrm{CO}_{2\mathrm{ocean}}) \cdot (\mathrm{k}/\mathrm{D}_{\mathrm{ML}})^{-1}$. The carbon system thermodynamic equations give a value of about 20 for $(\partial \mathrm{DIC}/\partial \mathrm{CO}_{2\mathrm{ocean}})$. Thus, the mixed layer equilibration time for CO_2 is about 8 months for a 50 m thick layer. This time scale is too long for oceanic processes to have a significant impact on the atmospheric CO_2 seasonal time scale variability.

Later we shall show some atmospheric oxygen measurements. The appropriate time scale for equilibration of O_2 produced by photosynthesis and consumed by remineralization is the aforementioned time of about two weeks. Thus, atmospheric O_2 shows a far larger seasonal signal than one would infer from the predominantly terrestrial CO_2 variations, and the Southern Hemisphere seasonality is of comparable magnitude to that in the Northern Hemisphere.

It is important to recall that the equilibration of the oceanic mixed layer with the atmosphere is rapid enough that gas exchange is not a rate limiting step for uptake of a longer time scale atmospheric perturbation such as the addition of fossil CO_2. As noted previously, the rate limiting step in such cases is mixing of the perturbation from the mixed layer down into the deeper layers of the ocean.

There are also significant interannual variations in atmospheric CO_2 due to the global scale climate changes known as the El Niño-Southern Oscillation phenomenon (e.g., Keeling et al. 1989a). One of the most noticeable phenomena of El Niño periods is the reduction in Equatorial Pacific upwelling. This decreases the flux of CO_2 out of the Equatorial Pacific without affecting the oceanic sinks for this carbon. The net effect is to turn the ocean into a net sink for CO_2. However, this sink is more than counterbalanced by a terrestrial source which Keeling et al. (1989a) attribute to collapse of the Southeast Asian monsoon: net carbon fixation decreases because precipitation is lower in El Niño years. During non-El Niño periods the situation is reversed, thus leading to a long term oscillation with a several year time scale.

In the following sections we examine in more detail the two best documented time periods: the glacial-interglacial cycles of the last few hundred thousand years, and the time since the beginning of the industrial revolution.

Glacial–interglacial carbon cycle

There is abundant evidence in the sedimentary record that Earth's climate has varied throughout geologic time. In the most basic terms, natural climate variations are described as changes in average global temperatures and changes in the area of the continents covered by glaciers. Both these properties are expressed most elegantly in the oxygen isotope composition of the CaCO_3 skeletons of foraminifera in deep sea sediments. The ratio of $^{18}\mathrm{O}$ (0.2% natural abundance) to $^{16}\mathrm{O}$ (99.8 % natural abundance) is expressed in units of per mil (‰):

$$\delta^{18}\mathrm{O}\ (\text{per mil})$$
$$= [(^{18}\mathrm{O}/^{16}\mathrm{O})_{\text{sample}}/(^{18}\mathrm{O}/^{16}\mathrm{O})_{\text{reference}} - 1] \times 10^3$$

Oxygen isotopes are fractionated during many chemical reactions, and the fractionation is temperature dependent. CaCO_3 precipitated from sea water has a higher $\delta^{18}\mathrm{O}$ than the water, and the $^{18}\mathrm{O}$ enrichment increases as sea water temperature decreases. Glaciers grow by the transfer of water from ocean to ice sheets. Oxygen isotope fractionation occurs when water in air forms rain or snow and causes glacial ice to have a $\delta^{18}\mathrm{O}$ much less than that of sea water. By mass balance, the $\delta^{18}\mathrm{O}$ of sea water must increase. High values for the $\delta^{18}\mathrm{O}$ of foraminifera of a certain age imply cold sea water temperatures and large glaciers, while low $\delta^{18}O$ values indicate warm temperatures and small glaciers.

$\delta^{18}O$ values for foraminifera during the last 100×10^6 years are plotted vs. age in Fig. 11a. These data show that, as indicated above, Earth's climate in polar and temperate regions, which was very warm during the Cretaceous, has been cooling (slowly and with reversals) ever since. Decreasing levels of atmospheric CO_2, associated with a slower rate of tectonic activity, are thought to be one process responsible for this long term climate deterioration. The slowly shifting position of the continents (i.e., continental drift) is thought to be the other. 100×10^6 years ago, the continents were aligned in a way that would allow the atmosphere and oceans to have transported much more heat than today from low to high latitudes (Barron and Washington 1985).

During the last hundred million years, and during earlier times as well, much of the variance in climate has been periodic. Fluctuations in indicators of past climates, such as the $\delta^{18}O$ of forams, can be described by sine waves with periods of 19 kyr (thousand years), 23 kyr, and 41 kyr (e.g. Imbrie et al. 1992). These periods correspond to periods of variation in the orientation of Earth as it orbits the sun, the so-called 'Milankovitch' cycles. The Earth's axis of spin is tilted with respect to the plane of its orbit. The tilt varies from 21 to 24° with a period of 41 kyr. The Earth's axis precesses (wobbles) about a line perpendicular to the plane of its orbit around the sun and going through the center of the Earth. Earth precesses with periods of about 19 and 23 kyr. These so called orbital changes do not affect the total amount of the sun's radiation intercepted annually by the Earth, but they do change seasonality. For example, when the tilt of the Earth's axis increases, temperate and boreal areas are pointed more towards the sun in summer, and days are warmer during that season. These changes in seasonality have profound effects on climate. For example, warm summers at high latitudes cause ice sheets to melt, and warm summers at low latitudes heat the Tibetan plateau and strengthen the summer (southwest) monsoon in India and the Arabian Sea. Such effects are manifested in the strong periodicities of 19, 23, and 41 kyr which are so prominent in records of global climate change throughout geological time. Climate changes associated with these periodicities are superimposed on the long-term cooling trend, discussed above, which occurred during the last 100×10^6 years.

During the last ~700 kyr B.P. (before present), Earth's climate has varied with a periodicity of about 100 kyr, as well as with the shorter periodicities described above (Fig. 11b). The 100 kyr periodicity tends to be sawtooth rather than sinusoidal in nature (Broecker and Donk 1970), with long coolings and an increase in the glaciated area of the Earth's surface followed by rapid warmings and terminations of glaciation. The origin of the 100 kyr cycle is hotly debated. Imbrie et al. (1992), among others, invoke orbital variations (the eccentricity of Earth's orbit around the sun varies with this period), while Saltzman and Sutera (1984) for example, suggest that this periodicity is fixed by the interaction of various elements of Earth's climate system.

The observation that cycles of Earth's climate have the same period as orbital variations is compelling evidence that these variations pace climate change (Hays et al. 1976). However, one cannot invoke orbital variations alone to account for the difference between glacial and interglacial climates. First, as noted above, orbital variations affect only the seasonal distribution of radiation at the Earth's surface, not its average value. Second, some seasonal changes induced by insolation are out of phase between the two hemispheres (i.e., precession causes warm northern hemisphere summers to accompany cold southern hemisphere summers), but glacial/interglacial climate change is synchronous between the hemispheres. Therefore, we need to invoke other factors in explaining glacial–interglacial changes in climate.

The most important such factors appear to be ocean circulation, albedo, and the atmospheric concentration of greenhouse gases. The flow of warm water northward in the North Atlantic Ocean is much reduced during glacial periods, maintaining Greenland, eastern North America, and northern Eurasia in a condition favorable to the growth and maintenance of ice sheets. Dur-

15.

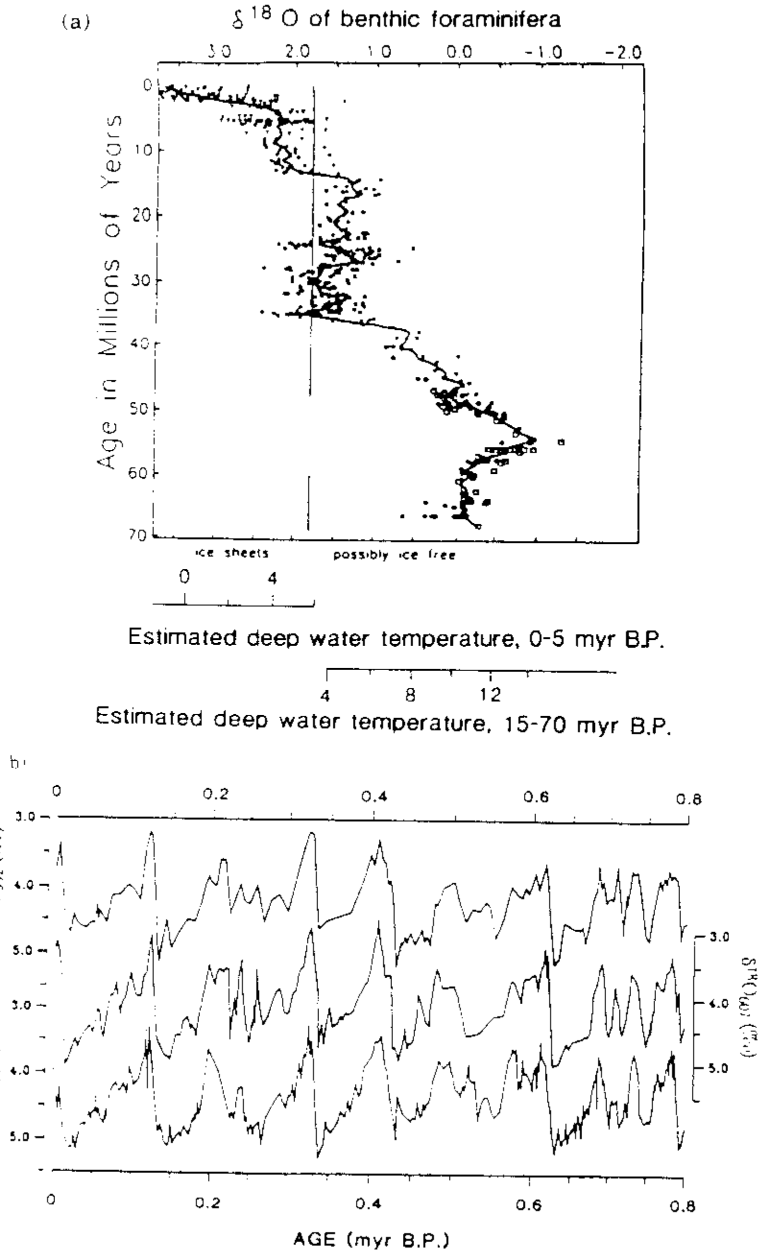

Fig. 11. (a) δ^{18}O of benthic foraminifera from the Atlantic Ocean vs. age from 0–70 myr B.P. (million years before present) (Miller et al. 1987). Benthic foraminifera are those living on the ocean floor. There δ^{18}O expresses Earth's climate in that it depends on the isotopic composition of seawater (which in turn depends on the volume of the continental ice sheets) and the temperature of the water in which the foraminifera grow. δ^{18}O increases as ice volume rises and temperature falls. The record in this figure thus reflects a (mostly) stepwise deterioration in climate resulting from the growth of ice sheets and the fall of polar temperatures, where the deep waters of the ocean are in contact with the surface. The upper temperature scale on the bottom of the graph corresponds to the modern isotopic composition of seawater, which the lower temperature scale corresponds to the isotopic composition seawater would have had when climate was warmer and the landmasses were free of large ice sheets. (b) δ^{18}O of benthic foraminifera from 3 North Atlantic Ocean deep sea sediment cores vs. age from 0–0.8 myr B.P. (from Raymo et al. 1990). High δ^{18}O values reflect large continental ice volume and cold temperatures of deep ocean waters, while low δ^{18}O values reflect small ice volume and warmer temperatures. These records are very similar to many other records from deep sea sediment cores taken throughout the global ocean. Note the sawtooth pattern characterizing much of the records, with long periods of cooling followed by rapid warming.

present)
that it
and the
cord in
of polar
ttom of
to the
ets. (b)
ymo et
w $\delta^{18}O$
eep sea
th long

ing glacial periods, large ice sheets reflect an important fraction of the sun's radiation back to space, thereby maintaining a cold climate. Finally, during glacial periods, the atmospheric concentration of CO_2 and other greenhouse gases is lower.

Our knowledge of glacial–interglacial variations in greenhouse gas concentrations comes from studies of the trapped gas content of samples from ice cores drilled in polar regions. As snow falls on a glacier, it becomes buried to progressively greater depths and is compacted by the overburden. By a depth of 50–100 m below the surface, the compaction is great enough that individual crystals of ice are sintered together, trapping an amount of air comprising about 10% of the volume of the enclosing ice. This air is nearly identical in composition to the contemporaneous atmosphere. The ice, and its contained air, will continue to be buried, but will reside in the ice sheet for very long periods before being transported to the oceans. By drilling through the thickest ice sheets in Greenland and Antarctica, we have recovered 7 deep ice cores extending back in time as far as 250 kyr or more. Melting or milling ice samples in a vacuum releases the trapped gases and allows us to collect samples of trapped air for analysis (Raynaud et al. 1993).

In Fig. 12, we plot the CO_2 concentration of air (as measured in the Vostok ice core) vs. age. We also plot the temperature at Vostok, inferred from the isotopic composition of the ice, and the isotopic composition of sea water, which is a measure of ice volume. In general, low atmospheric CO_2 concentrations are contemporaneous with cold temperatures and large volumes of continental ice. Many other indicators of cold climate vary in a similar way.

CO_2 concentrations at Vostok are about 180–190 ppmV during glacial times and 280 ppmV during 'pre-industrial times' of the present interglacial period in which we live. This change in CO_2 concentration alone would account for a change of roughly 1 °C in global average temperature. Feedbacks associated with the atmospheric concentration of water vapor (itself a greenhouse gas), changes in cloud cover (which affect the fraction of incoming solar radiation reflected back to space, and variations in the extent of (reflective) sea ice and snow cover amplify direct radiative forcing by CO_2 alone. The global temperature change attributable to glacial–interglacial CO_2 variations is about 2 °C, or 40–50% of the global temperature change of about 5 °C which occurred between glacial and interglacial times (Lorius et al. 1990).

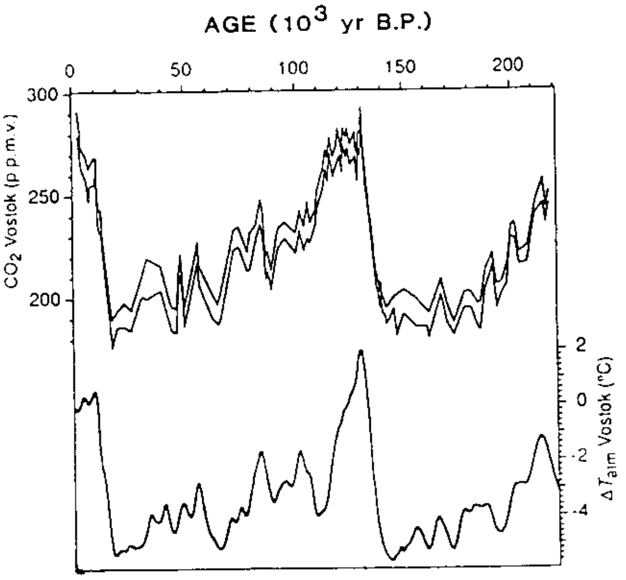

Fig. 12. CO_2 concentration of air and relative temperature at Vostok Station, East Antarctica, vs. age before present in thousands of years (from Jouzel et al. 1993). The CO_2 concentration is determined by the analysis of air trapped in old ice, and relative temperature is deduced from the oxygen or hydrogen isotopic composition of the ice. Note warm periods at about 220 000, 130 000 and 0–10 000 years before present characterized by warmer temperatures at Vostok, low $\delta^{18}O$ of benthic foraminifera, and high concentrations of atmospheric CO_2.

The geochemical causes of variations in the CO_2 concentration of air are currently a matter of vigorous debate. Two basic explanations have been proposed to explain the glacial–interglacial difference. The first is that biological productivity was enhanced during glacial times, so that organisms near the sea surface removed more CO_2 from the atmosphere and, by sinking, carried it to the deep ocean. Knox and McElroy (1984), Sarmiento and Toggweiler (1984), and Siegenthaler and Wenk (1984), have emphasized the importance of the Southern Ocean in this regard, because this region of the ocean contains a very large nutrient pool that would allow enhanced production if other necessary ingredients were supplied (cf. Table 2). The second is that the oceans might have been more alkaline, thereby drawing down atmospheric CO_2 as required by the physical chemistry of the carbonate system. Boyle (1988), for example, has presented evidence that the deep glacial oceans contained a higher concentration of metabolic CO_2 than the modern ocean. He argued that this would have led to increased dissolution of $CaCO_3$ from sea floor sediments and, therefore a higher sea water alkalinity. The higher alkalinilty would lower the partial pressure of CO_2 in the surface ocean and, hence, in the atmopshere. Many variations on these hypotheses have been proposed, along with intriguing discussions of the detailed behavior of CO_2 in the oceans and atmosphere during the transitions between glacial and interglacial climates (e.g., Broecker and Denton 1990).

An important related question is the role of CO_2 in inducing natural climate change. Several lines of evidence suggest that, during the penultimate glacial termination (at about 130 kyr B.P.), the atmospheric CO_2 concentration began rising about 3 kyr before the ice sheets melted (Sowers et al. 1991, Curry and Crowley 1987), suggesting that radiative forcing may have helped trigger the end of the ice age. During the last termination (beginning about 17 kyr B.P.), CO_2 rose simultaneously with the melting of the ice sheets and the rise in sea level. At the present time, we recognize that orbital variations, greenhouse gas variations, ocean circulation changes, and certain other effects drive glacial–interglacial climate change, but we do not understand how these forcings interact to produce the changes one observes.

Anthropogenic perturbations to the carbon cycle

Figure 13 shows atmospheric pCO_2 over the last thousand years. The primary aspect of this figure which will be discussed below is the large 27% increase that has occurred since the beginning of the industrial revolution. However, equally dramatic from a carbon cycle point of view is the stability of CO_2 concentrations prior to the industrial revolution (variations are less than ±10 ppmV). The latter imply that the natural carbon cycle was very close to a steady state over a long time span that included several major climatic episodes such as the Medieval Warm Period and the subsequent Little Ice Age. The present climate is thought to be within the range of these climate episodes. It thus seems reasonable to assume that the impact of recent climate fluctuations on the natural global carbon cycle has been minimal.

The observed increase in atmospheric pCO_2 must have been accompanied by a substantial oceanic uptake. Figure 14a shows an estimate of

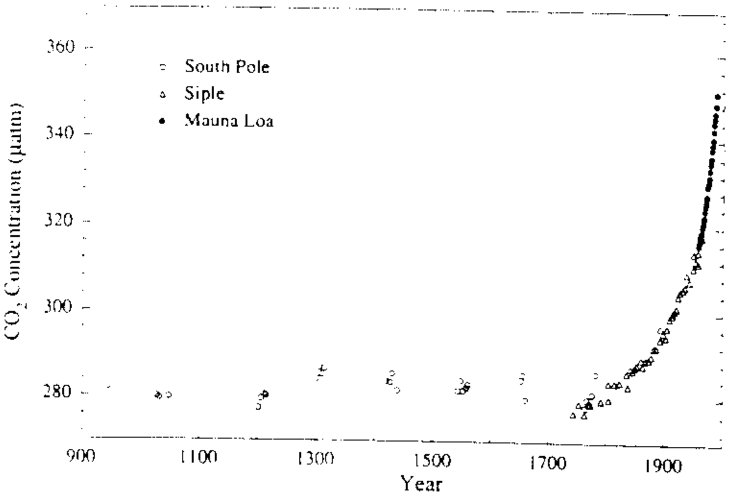

Fig. 13. Atmospheric carbon dioxide over the last 10^3 years as measured at Mauna Loa by C.D. Keeling (Boden et al. 1991), Siple Station by Neftel et al. (1985) and Friedli et al. (1986), and South Pole by Siegenthaler et al. (1988).

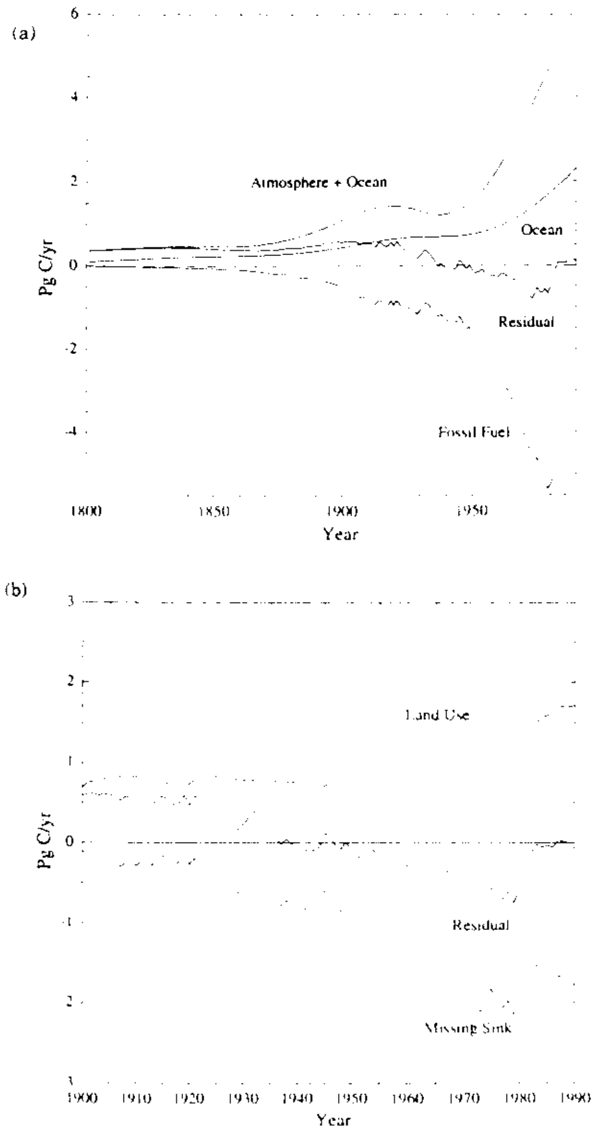

Fig. 14. (a) Time history of the anthropogenic CO_2 budget as determined by the ocean model of Sarmiento et al. (1992), combined with the atmospheric observations of Fig. 13, and the fossil fuel production history (Marland et al. 1989). The residual curve is thought to be due primarily to terrestrial processes. (b) Estimated net release of CO_2 to the atmosphere resulting from land use changes (R. Houghton 1992) compared with the residual from (a). The 'missing' sink is estimated by differencing the residual and land use terms.

the cumulative magnitude of this uptake as obtained by a three-dimensional ocean general circulation model following the technique of Sarmiento et al. (1992). The figure also shows the industrial release of CO_2 by fossil fuel burning and cement production as estimated from records of fuel and cement production. The release of fossil CO_2 to the atmosphere differs from the total increase in the atmosphere and ocean by a relatively modest amount. This difference reflects slow net release or uptake of CO_2 by the global terrestrial biosphere.

Figure 14b shows that estimates of CO_2 release to the atmosphere by land use changes (R. Houghton, personal communication) can account for most of the calculated net biosphere release until the early part of this century. In more recent decades, however, the estimated land use source is much larger than the net biosphere release. This discrepancy implies a so-called 'missing' sink which amounts today to a cumulative total of about 100 Pg of carbon. Table 3 shows the annual anthropogenic budget averaged over the last decade. We see from this that the missing sink is 1.8 ± 1.3 Pg of carbon per year. The very high uncertainty arises primarily from the uncertainty in land use change estimates. Despite this large uncertainty, biogeochemists take the missing sink very seriously and have put a great deal of effort into attempting to determine its nature.

Many of the papers in this volume explore mechanisms which could account for the missing sink. We thus limit ourselves here to a description of the temporal and spatial structure of this sink as inferred from a consideration of the carbon budget. First, however, a comment on why we believe the sink is most likely terrestrial in origin. A major reason is that measurements of $\delta^{13}C$ of CO_2 in air, discussed below, require a terrestrial sink. There is still some dispute about the accuracy of these measurements, but by far the best fit to them is obtained with models that put the missing sink into the terrestrial biosphere.

The other major reason is that ocean models of the potential impact on atmospheric CO_2 of modification of the oceanic carbon cycle show it to be very small (cf. Table 2). Even the most dramatic scenarios, such as total depletion of surface nutrients throughout the entire Southern Ocean, can only remove of order 70 ppmV of carbon from the atmosphere over a period of a century. Examination of the potential impact of the Equatorial Pacific, North Pacific, and North

Atlantic can account for far less removal, and coastal regions appear to have only a modest potential impact as well (Orr and Sarmiento 1992). There is no observational evidence to suggest that changes of such a magnitude have occurred anywhere in the ocean where their impact on atmospheric CO_2 would be sufficient to account for the missing sink.

Despite the large uncertainty in the missing sink, one cannot help but be intrigued by its strong correlation with the increasing level of CO_2, as well as with the temperature record since about 1950 as shown in Fig. 15. Prior to 1950 the correlation with temperature is of the opposite sign, but the CO_2 increase by 1950 was only about 40% of the total increase to the present time. Potential mechanisms for this correlation are explored in various of the following papers in this issue.

An additional strong hint as to the nature of the missing sink is provided by an estimate of its spatial distribution during the last decade. In a pair of pathbreaking papers Keeling et al. (1989b) and Tans et al. (1990) showed how one could use the north-south atmospheric pCO_2 gradients together with atmospheric transport models to estimate the spatial distribution of all the carbon sources and sinks in combination. Subtracting off other sources and sinks for which we have some knowledge of the spatial distribution led both Tans et al. and Keeling et al. to conclude that a very large fraction of the missing sink is in Northern Hemisphere temperate latitudes. Since then additional such studies have been carried out, of which the work by Enting et al. (1993) is perhaps most notable in that it uses a data fitting approach which makes effective use of all observational constraints and gives error estimates.

Variations in the carbon isotopic composition of ($\delta^{13}C$) of CO_2 in air, and in the ratio of O_2/N_2 in air, provide additional information about the anthropogenic carbon balance. The $\delta^{13}C$ of CO_2in air varies mainly because organic matter has a lower ratio of $^{13}C/^{12}C$ than CO_2in air or total CO_2 dissolved in seawater. Addition of CO_2 to air by the burning of fossil fuel or biomass thus causes the $\delta^{13}C$ of atmospheric CO_2 to decrease. Removal of CO_2 by plant growth causes $\delta^{13}C$ to rise, because plants assimilate ^{12}C preferentially. Release or uptake of CO_2 by the oceans leaves the $\delta^{13}C$ of air

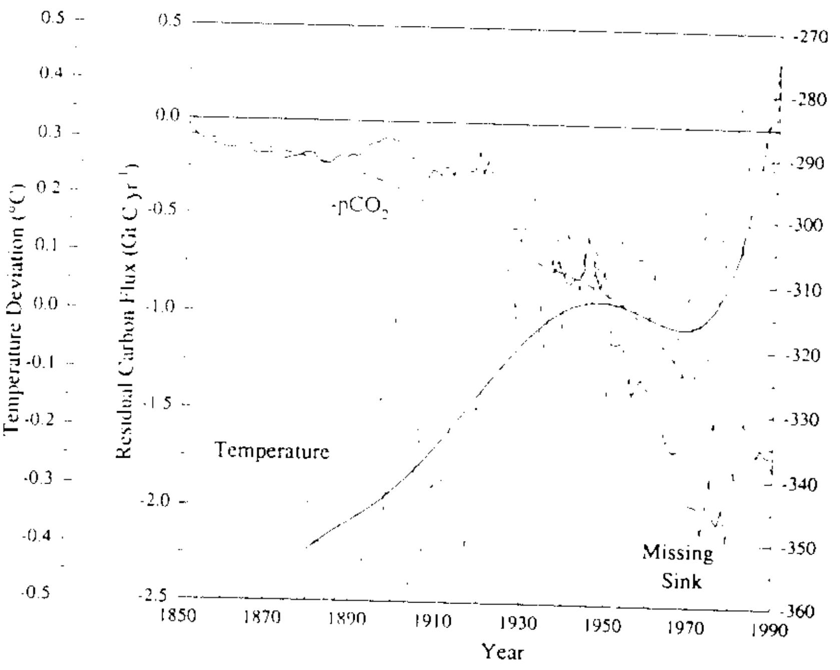

Fig. 15. 'Missing' carbon sink compared with the CO_2 data of Fig. 13, and an updated temperature history of Hansen and Lebedeff (1987).

---

unch
these
the
atmo
addit
pher
fuels
$\delta^{13}C$
latitu
amin
term
CO_2
the

W
the
cent
refle
We
and
carb
mos
in a
cycl
Firs
carl
cate
fuel
diss
Gig
anc
occ
CC
anc
tha
yea
car
atn
the
of
no
dis
the
tha

to
be
As
se.
of
oc

20.

unchanged or nearly so. In qualitative terms, these generalizations readily explain variations in the $\delta^{13}C$ of CO_2 in air. $\delta^{13}C$ in the global atmosphere is decreasing with time due to the addition of ^{13}C-depleted fossil fuel to the atmosphere. At any one time, burning of the fossil fuels mainly in the northern hemisphere causes $\delta^{13}C$ of CO_2 to be lower in temperate northern latitudes and to rise as one goes south. Examined in more detail, $\delta^{13}C$ allows us to determine whether regional sources and sinks of CO_2 are associated with the land biosphere or the ocean.

We can estimate fluxes of CO_2 into and out of the atmosphere from gradients in the CO_2 concentration of air in time or space (higher CO_2 reflects addition, lower CO_2 indicates removal). We can use $\delta^{13}C$ data to infer whether sources and sinks of CO_2 are associated with organic carbon. Keeling et al. (1989a,b) have made the most detailed studies of the distribution of CO_2 in air and its implications for the global carbon cycle. Three important results have emerged. First, data on variations in the concentration and carbon isotopic composition of CO_2 in air indicate that, around 1980, about 60% of the fossil fuel input remained as CO_2 in air and 40% dissolved in the ocean. To within about ±0.5 Gigatons of C, the land biosphere was in balance: release of CO_2 from deforestation occurred at about the same rate as enhanced CO_2 uptake by reforestation CO_2 fertilization, and other processes. Second, $\delta^{13}C$ data confirm that changing weather patterns during El Niño years can cause an increase in the net rate of carbon release from the land biosphere to the atmosphere. Third, the north-south gradient in the $\delta^{13}C$ of CO_2 in air indicates that the removal of CO_2 in temperate and boreal regions of the northern hemisphere, inferred from the CO_2 distribution in air, is due primarily to uptake by the ocean (mainly the North Atlantic) rather than by the land biosphere.

The changing $\delta^{13}C$ of seawater is transmitted to the ocean by chemical exchange of CO_2 between the atmosphere and surface seawater. As a result, the $\delta^{13}C$ of total dissolved CO_2 in seawater has been decreasing with time. The rate of this decrease is related to the rate at which the oceans are taking up CO_2. Quay et al. (1992) first recognized that the oceanic $\delta^{13}C$ decrease could be used to constrain the anthropogenic CO_2 balance, and presented data on the change in the $\delta^{13}C$ of CO_2 in seawater between 1970 and 1990. They calculated that, during this period, the ocean was taking up CO_2 at the rate of 1.5 ± 0.4 Gt/yr, with 0.6 ± 0.4 Gt/yr going into the biosphere. Their mass balance was thus in rough agreement with other recent estimates. Broecker and Peng (1993) and Tans et al. (1993) have recently reinterpreted their data from other perspectives and suggested that uncertainties in oceanic CO_2 uptake rates estimated from this approach must be very large. The utility of seawater $\delta^{13}C$ data in constraining the anthropogenic CO_2 mass balance is a matter of vigorous discussion.

Another emerging approach to constraining the anthropogenic carbon balance comes from studies of the changing O_2 concentration of air (Keeling 1988). This approach invokes the fact that O_2 is so insoluble in the oceans that air-sea exchange does not affect the inventory of this gas in the atmosphere over times longer than a year or so. Burning of fossil fuel and deforestation consume O_2, while enhanced growth of the land biosphere produces O_2 (along with biomass). The change in the O_2 concentration of air reflects the sum of the fluxes associated with these three processes. By measuring the rate of change of the O_2 concentration of air and subtracting the (known) rate at which O_2 is consumed by burning fossil fuel, one can calculate the net rate of change of the biomass of the land biosphere. These rates, together with the rate of increase of the CO_2 concentration of air, constrain the rate at which fossil fuel CO_2 dissolves in the ocean.

The natural processes of photosynthesis and respiration in undisturbed land ecosystems turn over much larger amounts of carbon and O_2 than anthropogenic perturbations (cf. Fig. 4 and Table 3). However, natural rates of photosynthesis and respiration are almost perfectly in balance over the course of a year. The same is true of marine ecosystems. These natural processes cause the O_2 concentration of air to vary on a seasonal time scale, and even on interannual time scales in response to perturbations such as El Niño, but the signal that will predominate over the long term is that due to the anthropogenic perturbation.

Keeling and Shertz (1992) and more recently Bender et al. (1993) measured the O_2/N_2 ratio of air at La Jolla, California, and other locations (Fig. 16). Units of per meg are defined by the equation

$$\delta(O_2/N_2),\ \text{per meg} = [(O_2/N_2)\ \text{sample}\ (O_2/N_2)\ \text{standard} - 1] \times 10^6$$

For reference, a change of about 5 per meg corresponds to approximately 1 ppmV O_2 out of 210,000. Between 1989 and 1992, the O_2/N_2 ratio decreases at the rate of 18 per meg per year. Keeling and Shertz calculated that this decrease corresponds to a net flux of 0.2 ± 1.7 Gt C/yr CO_2 out of the land biosphere, and 2.5 ± 1.7 Gt C/yr CO_2 from the atmosphere into the oceans. These fluxes are in line with other recent estimates, but again uncertainties are large. It will take another 5–10 years before O_2/N_2 data will constrain anthropogenic carbon fluxes within small uncertainties.

Projections of future increases of CO_2 are frought with great uncertainty resulting primarily from the wide range of possible emission scenarios. This can perhaps be best illustrated by the attempts of the IPCC to provide authoritative estimates of future CO_2 growth rates and resulting climate change as a guide to decision makers (Houghton et al. 1990). Their 1990 report gave a wide range of scenarios ranging from one which assumed that fossil emissions continued at present (i.e., 1990) levels, to a 'business as usual' scenario which projected present growth rates of fossil fuel burning into the future, allowing for the impact of dwindling fossil fuel reserves as time goes on. Models of these two scenarios give future CO_2 levels a century from now of about 500 ppmV in the low emission scenario versus 800 ppmV in the high emission scenario (Sarmiento and Orr 1991).

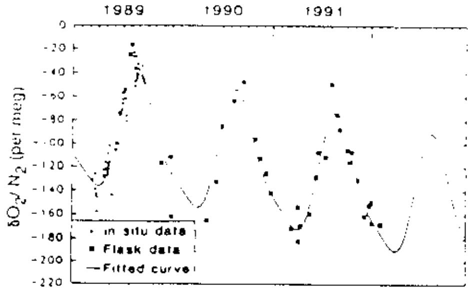

Fig. 16. O_2/N_2 ratio in air at La Jolla, California vs. time from 1989–1992. Units of per meg are defined in the text. The ratio increase in the summertime as land and marine plants grow, producing O_2, and falls in the winter due to respiration. Note the long term decrease in the O_2/N_2 ratio of air, which mainly reflects anthropogenic consumption of O_2 due to the burning of fossil fuels.

The political landscape has evolved significantly since the time that the IPCC 1990 report was prepared. In particular, most developed countries have recognized the importance of controlling emissions at levels that will not permit CO_2 to rise above concentrations that would cause harmful climate change. Although it is difficult to define what CO_2 concentration levels will cause harmful climate change, this change in views does suggest an alternative strategy for scientists to provide input to decision makers. IPCC is preparing a new report prescribing a range of future upper limit atmospheric CO_2 concentrations, and calculating allowable emissions by model calculations of how much CO_2 can be taken up by the oceans, terrestrial biosphere, and atmosphere under these particular scenarios (Enting et al. 1994).

Figure 17 shows the IPCC 1994–1995 scenarios as well as calculations by Sarmiento, Le Quéré and Pacala (in preparation) of oceanic uptake for two of them. The outstanding feature which is of relevance to the topic of this special issue is the large contribution to the carbon budget by the missing sink. During the last decade, the missing sink accounts for a third of the fossil emissions and more than a quarter of the combined land use and fossil emissions. Projections of the future behavior of this missing sink are thus a major uncertainty in the IPCC 1994–1995 emission scenarios.

Acknowledgements

We appreciate the assistance of Jason Olszewski in preparation of the manuscript. J.L.S. was supported by the National Science Foundation Joint Global Ocean Flux Program (OCE-

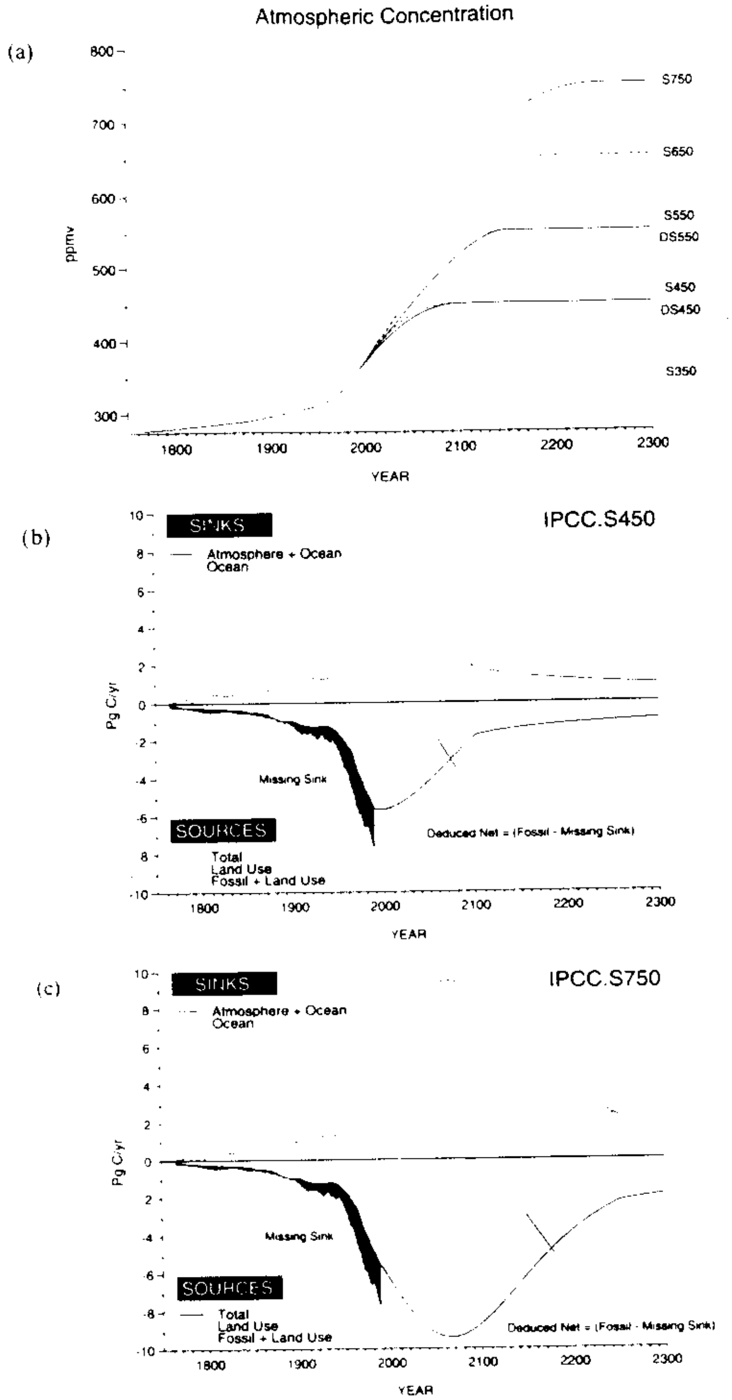

Fig. 17. (a) Future atmospheric CO_2 scenarios developed for the IPCC 1994–1995 study (Enting et al. 1994). The line labels give the assymptotic CO_2 concentration. S stands for 'stabilization', D is for scenarios in which the approach to the stabilized CO_2 value is 'delayed'. (b) and (c) Future emission scenarios consistent with the IPCC 1994–1995 450 ppmV and 750 ppmV atmospheric CO_2 scenarios. The oceanic uptake, which is depicted as a sink, is predicted by an ocean model (Sarmiento, Le Quéré and Pacala, in preparation). The annual atmospheric increase deduced from (a) is summed to the oceanic uptake estimate to give a combined sink. This combined sink is depicted as a combined source in the lower half of the figure. The land use estimate in the lower part of the figure is based on Houghton (1992) prior to 1990, and on Enting et al. (1994) after 1990. The fossil fuel production source of Marland et al. (1989) is summed to the land use source to give the total sources that must be accounted for prior to 1990. These are greater than the combined atmosphere and ocean sink by an amount which is referred to as the missing sink. Note that the missing sink is a very substantial portion of the fossil fuel emissions. The future permissible emissions would be far larger if the missing sink continues to play a role.

23.

9314707) and by the US Department of Energy under contract DE-FG02-90ER61052. M.L.B. gratefully acknowledges financial support from NSF grant ATM 9214776 and EPA IAG DW49935603-01-0.

References

Arthur MA, Allard D and Hinga KR (1991) Cretaceous and Cenozoic atmospheric carbon dioxide variations and past global climate change. Geol Soc Am Ann Meeting Abstr A: 178

Bainbridge AE (1976) Geosecs Atlantic Expedition, Sections and Profiles Vol 2. US Government Printing Office, Washington DC

Barron EJ (1983) A warm, equable Cretaceous: The nature of the problem. Earth Sci Rev 19: 305–338

Barron EJ and Washington WM (1985) Warm Cretaceous climates: High atmospheric CO_2 as a plausible mechanism. In: Sundquist ET and Broeker WS (eds) The Carbon Cycle and Atmospheric CO_2: Natural Variations Archean to Present, pp 546–553. American Geophysical Union, Washington DC

Bender M, Tans P and Ellis T (1993) The distribution of O_2 in the Southern Hemisphere air: Implication for the ocean carbon cycle. 4th Int Conf on CO_2, WMO/TD – No 56, World Meteorological Organization Global Atmosphere Watch, No 89, Geneva

Berner RA (1991) A model for atmospheric CO_2 over phanerozoic. Am J Sci 291: 339–376

Berner RA (1992) Palaeo-CO_2 and climate. Nature 358: 114

Berner RA, Lasaga AC and Garrels RM (1983) The carbonate-silicate geochemical cycle and its effect on atmospheric carbon dioxide over the past 100 million years. Am J Sci 283: 641–683

Boden TA, Sepanski RJ and Stoss FW (eds) (1991) Trends '91: A compendium of data on global change. ORNL CDIAC-46. Carbon Dioxide Information Analysis Center, Oak Ridge National Laboratory, Oak Ridge, Tennessee, 700 pp

Boyle EA (1988) Vertical oceanic nutrient fractionation and glacial/interglacial CO_2 cycles. Nature 331: 55–56

Broecker WA and Denton GH (1990) What drives glacial cycles? Scientific American 262: 49–56

Broecker WS and Donk JV (1970) Insolation changes, ice volumes, and the ^{18}O record in deep sea cores. Rev Geophys Space Phys 8: 169–198

Broecker WS and Peng TH (1993) Evaluation of the ^{13}C constraint on the uptake of fossil fuel CO_2 by the ocean. Global Biogeochemical Cycles 7: 619–626

Broecker WS and Takashashi T (1977) Neutralization of fossil fuel CO_2 by marine calcium carbonate. In: Anderson NR and Malahoff A (eds) The Fate of Fossil Fule CO_2 in the Oceans, pp 213–239. Plenum Press, New York

Brook GA, Folkoff ME and Box EO (1983) A world model of soil carbon dioxide. Earth Surf Processes Landforms 8: 79–88

Cerling TE (1991) Carbon dioxide in the atmosphere: Evidence from cenozoic and mesozoic paleosols. Am J Sci 291: 377–400

Cerling TE (1992) Use of carbon isotopes in paleosols as an indicator of the P(CO_2) of the paleoatmosphere. Global Biogeochem Cycles 6: 307–314

Cerling TE, Solomon DK, Quade J and Bowman JR (1991) On the isotope composition of carbon in soil carbon dioxide. Geochim Cosmochim Acta 55: 3403–3405

Chyba C (1987) The cometary contribution to the oceans of the primitive earth. Nature 330: 632–635

Conway TJ, Tans PP and Waterman LS (1991) In: Boden TA, Sepanski RJ and Stoss FW (eds) Trends '91, pp 44–143. Vol ORNL/CDIAC-46, ESD Publication No 3746, Carbon Dioxide Information Analysis Center, Environmental Sciences Division, Oak Ridge National Laboratory, Oak Ridge, TN

Craig H, Broecker WS and Spencer D (1981) Geosecs Pacific Expedition, Vol 4, Sections and Profiles. US Government Printing Office, Washington DC

Curry WB and Crowley TJ (1987) The $d^{13}C$ of equatorial Atlantic surface waters: Implications for ice age pCO levels. Paleoceanography 2: 489–517

Enting IG, Trudinger CM, Francey RJ and Granek H (1993) Synthesis inversion of atmospheric CO_2 using the GISS tracer transport model. CSIRO Aust Div Atmos Res Tech Pap 29: 1–44

Enting IG, Wigley TML and Heimann M (1994) Assessment of the IPCC CO_2 modelling study, Technical Paper No 31 CSIRO Division of Atmospheric Research

Eppley RW (1972) Temperature and phytoplankton growth in the sea. Fish Bull 70: 1063–1085

Falkowski PG (1994) The role of phytoplankton photosynthesis in global biogeochemical cycles. Photosynth Res 39: 235–258 (this issue)

Freeman KH and Hayes JM (1992) Fractionation of carbon isotopes by phytoplankton and estimates of ancient CO levels. Global Biogeochem Cycles 6: 185–198

Friedli H, Lötscher H, Oeschger H, Siegenthaler U and Stauffer B (1986) Ice core record of the $^{13}C/^{12}C$ ratio of atmospheric carbon dioxide in the past two centuries. Nature 324: 237–238

Gaffin S (1987) Ridge volume dependence on seafloor generation rate and inversion using long term sealevel change. Am J Sci 287: 596–611

Hansen J and Lebedeff S (1987) Global trends of measured surface air temperature. J Geophys Res 92: 13345–13372

Hays JD, Imbrie J and Shackleton NJ (1976) Variations in the Earth's orbit: Pacemaker of the ice ages. Science 194: 1121–1132

Hellerman S and Rosenstein M (1983) Normal monthly wind stress over the world ocean with error estimates. J Phys Oceanogr 13: 1093–1104

Hollander DJ and McKenzie JA (1991) CO_2 control on carbon-isotpe fractionation during aqueous photosynthesis: A paleo-pCO_2 barometer. Geology 19: 929–932

Houghton JT, Jenkins GJ and Ephraums JJ (1990) Climate Change, The IPCC Scientific Assessment. Cambridge University Press, Cambridge

Houghton RA (1992) Effects of land-use change, surface temperature, and CO_2 concentration on terrestrial stores of carbon. Paper presented at the IPCC-sponsored International Workshop on Biotic Feedbacks in the Global Climatic System, Woods Hole, Massachusetts, October 26–29, 1992

abrie J, Boyle EA, Clemens SC, Duffy A, Howard WR et al. (1992) On the structure and origin of major glaciation cycles, 1. Linear responses to Milankovitch forcing. Paleoceanography 7: 701–738

ouzel J, Barkov NI, Barnola JM, Bender M, Chappellaz J, Genthon G, Kotlyakov VM, Lipenkov V, Lorius C, Petit JR, Raynaud D, Raisbeck G, Ritz C, Sowers T, Stievenard M, Yiou F and Yiou P (1993) Extending the Vostok ice-core record of paleoclimate to the penultimate glacial period. Nature 364: 407–412

Kasting JF (1985) Photo chemical consequences of enhanced CO_2 levels in Earth's early atmosphere. In: Sundquist ET and Broecker WS (eds) The Carbon Cycle and Atmospheric CO_2: Natural Variations Archean to Present, pp 612–622, Vol Geophysical Monograph 32. American Geophysical Union, Washington DC

Keeling CD, Bacastow RB, Carter AF, Piper SC, Whorf TP, Heimann M, Mook WG and Roeloffzen H (1989a) A three-dimensional model of atmospheric CO_2 transport based on observed winds: 1 Analysis of observation data. In: Peterson DH (ed) Aspects of Climate Variability in the Pacific and the Western Americas, AGU Monograph 55, pp 165–236. AGU, Washington DC

Keeling CD, Piper SC and Heimann M (1989b) A three-dimensional model of atmospheric CO_2 transport based on observed winds: 4 Mean annual gradients and interannual variations. In: Peterson DH (ed) Aspects of Climate Variability in the Pacific and the Western Americas, AGU Monograph 55, pp 305–363. AGU, Washington DC

Keeling RF (1988) Development of an interferometric oxygen analyzer for precise measurement to the atmospheric O_2 mole fraction. PhD thesis, Harvard University

Keeling RF and Shertz SR (1992) Seasonal and interannual variations in atmospheric oxygen and implications for the global carbon cycle. Nature 358: 723–727

Knox F and McElroy M (1984) Changes in atmospheric CO_2, influence of marine biota at high latitudes. J Geophys Res 89: 4629–4637

Lasaga AC, Berner RA and Garrels RM (1985) Fluctuations over the past 100 million years. In: Sundquist ET and Broecker WS (eds) The Carbon Cycle and Atmospheric CO_2: Natural Variations Archean to Present, pp 397–411, Geophysical Monograph 32. AGU, Washington DC

Levitus S (1982) Climatological Atlas of the World Ocean. Natl Oceanic and Atmos Admin, Boulder, CO

Levitus S, Conkright ME, Reid JL, Najjar RG and Mantyla A (1993) Distribution of nitrate, phosphate and silicate in the world oceans. Prog Oceanog 31: 245–273

Lorius C, Jouzel J, Raynaud D, Hansen J and Treut HI (1990) The ice-core record: Climate sensitivity and future greenhouse warming. Nature 347: 139–145

Maier-Reimer E and Hasselmann K (1987) Transport and storage of CO_2 in the ocean–an inorganic ocean circulation cycle model. Climate Dyn 2: 63–90

Marland G, Boden TA, Griffin RC, Huang SF, Kanciruk P and Nelson TR (1989) Estimates of CO_2 emissions from fossil fuel burning and cement manufacturing, based on the US Bureau of Mines cement manufacturing data, ORNL/CDIAC-25, NDP-030. Carbon Dioxide Information Analysis Center, Oak Ridge National Laboratory, Oak Ridge, TN

Miller KG, Fairbanks RG and Mountain GS (1987) Tertiary oxygen isotope synthesis, sea level history, and continental margin erosion. Paleoceanography 2: 1–19

Mora CI, Driese SG and Seager PG (1991) Carbon dioxide in the Paleozoic atmosphere: Evidence from carbon-isotope compositions of pedogenic carbonate. Geology 19: 1017–1020

Najjar R (1992) Marine biogeochemistry. In: Trenberth KE (ed) Climate System Modeling, pp 241–280. Cambridge University Press, Cambridge

Neftel A, Moor E, Oeschager H and Stauffer B (1985) Evidence from polar ice cores for the increase in atmospheric CO_2 in the past two centuries. Nature 315: 45–47

Orr JC and Sarmiento JL (1992) Potential of marine macroalgae as a sink for CO_2: Constraints from a 3-D general circulation model of the global ocean. Water, Air & Soil Pollution 64: 405–421

Quay PD, Tilbrook B and Wong CS (1992) Oceanic uptake of fossil fuel CO_2: Carbon-13 evidence. Science 256: 74–79

Raymo ME, Shackleton WF and Oppo DW (1990) Evolution of Atlantic-Pacific $\delta^{13}C$ gradients over the last 2.5 m.y. Earth Planet Sci Lett 97: 353–368

Raynaud D, Jouzel J, Barnola JM, Chappellaz J, Delmas RJ and Lorius C (1993) The ice record of greenhouse gases. Science 259: 926–934

Raven JA (1994) Carbon fixation and carbon availability in marine phytoplankton. Photosynth Res 39: 259–273 (this issue)

Saltzman B and Sutera A (1984) A model of the internal feedback systems involved in late Quaternary climatic variations. J Atmos Sci 41: 736–745

Sarmiento JL and Orr JC (1991) Three-dimensional simulations of the impact of Southern Ocean nutrient depletion on atmospheric CO_2 and ocean chemistry. Limnol Oceanogr 36: 1928–1950

Sarmiento JL and Siegenthaler U (1992) New Production and the Global Carbon Cycle. In: Falkowski PG and Woohead AD (eds) Primary Productivity and Biogeochemical Cycles in the Sea, pp 317–332. Plenum Press, New York

Sarmiento JL and Toggweiler JR (1984) A new model for the role of the oceans in determining atmospheric pCO_2. Nature 308: 621–624

Sarmiento JL, Orr JC and Siegenthaler U (1992) A perturbation simulation of CO_2 uptake in an ocean general circulation model. J Geophys Res 97: 3621–3646

Shine KP, Derwent RG, Wuebbles DJ, Morcrette J-J (1990) Radiative forcing of climate. In: Houghton JT, Jenkins GJ and Ephraums JJ (ed) Climate Change, The IPCC Scientific Assessment, pp 41–68. Cambridge University Press, Cambridge

Siegenthaler U (1986) Carbon dioxide: Its natural cycle and anthropogenic perturbation. In: Buat-Ménard P (ed) The

Role of Air-Sea Exchange in Geochemical Cycling, pp 209–248. D Reidel, Dordrecht

Siegenthaler U and Sarmiento JL (1993) Atmospheric carbon dioxide and the ocean. Nature 365: 119–125

Siegenthaler U and Wenk T (1984) Rapid atmospheric CO_2 variations and ocean circulation. Nature 308: 624–625

Siegenthaler U, Friedli H, Loetscher H, Moor E, Neftel A, Oeschger H and Stauffer B (1988) Stable-isotope ratios and concentration of CO_2 in air from polar ice cores. Ann Glaciol 10: 1–6

Sowers TM, Bender M, Raynaud D, Korotkevich YS and Orchardo J (1991) The $d^{18}O$ of atmospheric O_2 from air inclusions in the Vostok ice core: Timing of CO_2 and ice volume changes during the penultimate deglaciation. Paleoceanography 6: 679–696

Tans PP, Fung IY and Takahashi T (1990) Observational constraints on the global atmospheric CO_2 budget. Science 247: 1431–1438

Tans PP, Berry JA and Keeling RF (1993) Oceanic $^{13}C/^{12}C$ observations: A new window on ocean CO_2 uptake. Global Biogeochemical Cycles 7: 353–368

Taylor DW and Hickey LJ (1990) An Aptian plant with attached leaves and flowers: Implications for angiosperm origin. Science 247: 702–704

Thomason JR, Nelson ME and Zakrezewski RJ (1988) A fossil grass (Gramineae: Chloridoideae) from the Miocene with Kranz anatomy. Science 233: 876–878

Toggweiler JR, Dixon K and Bryan K (1989) Simulation of radiocarbon in a coarse-resolution world ocean model. 1. Steady state prebomb distributions. J Geophys Res 94: 8217–8242

Volk T (1989) Rise of angiosperms as a factor in long-term climate cooling. Geology 17: 107–110

Volk T and Hoffert MI (1985) Ocean carbon pumps: Analysis of a relative strengths and efficiencies in ocean-driven atmospheric CO_2 changes. In: Sundquist ET and Broecker WS (eds) The Carbon Cycle and Atmospheric CO_2: Natural Variations Archean to Present, pp 99–110. Geophysical Monograph 32, American Geophysical Union, Washington, DC

Watson RT, Rodhe H, Oeschger H and Siegenthaler U (1990) In: Houghton JT, Jenkins GJ and Ephraums JJ (eds) Climate Change, The IPCC Scientific Assessment, pp 1–40. Cambridge University Press, Cambridge

Wilkinson BH and Walker JCG (1989) Phanerozoic cycling of sedimentary carbonate. Am J Sci 289: 525–548

Yapp CJ (1992) Ancient atmospheric CO_2 pressures inferred from natural goethites. Nature 355: 342–344